

## REPORTS

## INDUCED SEISMICITY

# High-rate injection is associated with the increase in U.S. mid-continent seismicity

M. Weingarten,<sup>1\*</sup> S. Ge,<sup>1</sup> J. W. Godt,<sup>2</sup> B. A. Bekins,<sup>3</sup> J. L. Rubinstein<sup>3</sup>

An unprecedented increase in earthquakes in the U.S. mid-continent began in 2009. Many of these earthquakes have been documented as induced by wastewater injection. We examine the relationship between wastewater injection and U.S. mid-continent seismicity using a newly assembled injection well database for the central and eastern United States. We find that the entire increase in earthquake rate is associated with fluid injection wells. High-rate injection wells (>300,000 barrels per month) are much more likely to be associated with earthquakes than lower-rate wells. At the scale of our study, a well's cumulative injected volume, monthly wellhead pressure, depth, and proximity to crystalline basement do not strongly correlate with earthquake association. Managing injection rates may be a useful tool to minimize the likelihood of induced earthquakes.

The injection of fluids into the subsurface has been known to induce earthquakes since the mid-1960s (1–3). However, few additional cases of earthquakes induced by wastewater injection have been documented until 2009 (4). The hazard from these earthquakes was considered small because they were infrequent and not expected to be large (largest observed prior to 2011 was the *M* 4.9 Rocky Mountain Arsenal earthquake in 1967) (4–6). The central and eastern United States (CEUS) has seen an unprecedented increase in earthquake rate since 2009, and many of these earthquakes are believed to be induced (7). Along with the increased rate, several damaging earthquakes have occurred such as the 2011 magnitude (*M*) 5.6 Prague, Oklahoma, earthquake (8, 9), the 2011 *M* 5.3 Trinidad, Colorado, earthquake (10), the 2012 *M* 4.8 Timpson, Texas, earthquake (11), and the 2011 *M* 4.7 Guy, Arkansas, earthquake (12). The increased earthquake rate and occurrence of multiple damaging earthquakes has prompted the scientific community to refocus efforts to understand the hazard posed by injection-induced earthquakes (13).

The sudden appearance of several large, potentially induced earthquakes led to many site-specific case studies (4). These case studies examined the operation of injection wells in close proximity to the earthquakes, showing a link between the timing and location of injection and seismicity (12, 14–18). Though useful to understand the individual systems in which these earthquakes occurred, broader-scale studies are needed to

understand the phenomenon as a whole. One previous study examined earthquakes in Texas's Barnett Shale region and found that earthquakes are commonly located near wells injecting more than 150,000 barrels per month (19). However, to fully understand the possibility of induced seismicity associated with a given injection well, we must analyze a range of geologic, hydrogeologic, and operational differences between injection wells that are potentially associated with earthquakes and those that are not.

We examined the location and timing of earthquakes and their relationship to the location and operation of injection wells across the CEUS (Fig. 1). We compiled a database from publicly available sources that documents the location and operational parameters of underground injection control class II injection wells in the CEUS (Fig. 1 and table S1). Class II injection wells inject fluids associated with oil and gas production and are distinct from hydraulically fractured production wells (20). The database contained 187,570 wells as of December 2014, with 56% actively injecting fluid (Fig. 1) and the remaining 44% being inactive or abandoned. About 75% of the active class II injection wells operated for the purposes of enhanced oil recovery (EOR), whereas nearly all of the remaining wells were designated as salt water disposal (SWD) wells (fig. S1). EOR wells inject fluid into depleted oil reservoirs to increase oil production. SWD wells inject to dispose of waste fluids produced by oil and gas production, which would otherwise be hazardous to surface waters or underground sources of drinking water. Injection wells are geographically clustered in the basins and regions of major oil and gas operations. Texas, Oklahoma, Kansas, and Wyoming contain ~85% of all class II injection wells in the CEUS. The

spatial density of active SWD wells is highest ( $\geq 5$  wells per 5 km<sup>2</sup>) in the Fort Worth Basin of north-central Texas and the Mississippi Lime Play extending from north-central Oklahoma northward into central Kansas. The spatial density of active EOR wells is highest ( $\geq 5$  wells per 5 km<sup>2</sup>) in the Permian Basin of West Texas, the Fort Worth Basin, south-central Oklahoma, and southeastern Kansas (fig. S1).

We obtained earthquake location and magnitude data from the Advanced National Seismic System's comprehensive earthquake catalog (ANSS ComCat) (21). During the study period (1973 to 2014), we identified 7175 *M*  $\geq$  0.0 events in the catalog in the CEUS region (Fig. 2). Although the catalog is not complete down to *M* 0.0 during the study period, we treated all earthquakes as potentially induced events to capture the most comprehensive data set of associated earthquakes and injection wells. We used a magnitude of completeness of 3.0 when comparing associated versus nonassociated earthquakes through time (7).

We used spatial and temporal filtering methods to discriminate injection wells that may be associated with earthquakes from those that are probably not. We considered any earthquake within 15 km of an active injection well to be associated with that well. This distance of association is based upon the sum of a 5-km radius within which earthquakes are traditionally considered as potentially induced (22) and a 10-km estimate of the spatial uncertainty in earthquake epicenter location in the CEUS (23). We designed the temporal filter to include only injection wells active at the time of the spatially associated earthquake. Both filters could be considered conservative, because induced seismicity has been found tens of kilometers from injection wells (24) and also after a well is shut-in (25) owing to the injection prior to the well becoming inactive (4, 5). To analyze the sensitivity of our results to these filtering parameters, we also tested our analysis using spatial association distances of 5 and 10 km. This first-order analysis attempts to understand which basic well properties affect the likelihood of earthquake association.

We find 18,757 injection wells (~10% of all wells) associated with earthquakes in the CEUS after filtering, mostly in the states of Oklahoma and Texas (Fig. 1). The number of associated injection wells has tripled since the year 2000 (fig. S2). The spatiotemporal filter identifies every case of induced seismicity from class II injection wells documented in the literature for the CEUS region (table S2). We identify far more injection wells that are potentially related to earthquakes than those indicated by published cases. Of the wells that are associated with earthquakes, 66% are EOR wells. However, active SWD wells are more than 1.5 times as likely as active EOR wells to be associated with an earthquake, which accounts for their respective well totals (Fig. 1). The finding that SWD wells are preferentially associated with earthquakes likely resides with difference in well operation. SWD injection causes a net-positive reservoir pressure change, whereas EOR injection and extraction

<sup>1</sup>Department of Geological Sciences, University of Colorado, Boulder, CO, USA. <sup>2</sup>United States Geological Survey, Denver, CO, USA. <sup>3</sup>United States Geological Survey, Menlo Park, CA, USA. \*Corresponding author. E-mail: matthew.weingarten@colorado.edu

wells are typically operated in tandem with injection rates managed carefully to balance reservoir pressures (7).

Over the past four decades, more than 60% of all CEUS seismicity ( $M \geq 3.0$ ) is associated with injection wells using our filtering criteria (Figs. 2 and 3). Varying the spatial distance of association by several kilometers only changes this percentage by  $\pm 5\%$  (fig. S3). Before the year 2000, an average of  $\sim 20\%$  of all CEUS seismicity was associated with injection wells. The yearly percentage of associated earthquakes has risen sharply to  $\sim 87\%$  from 2011 to 2014 (Fig. 3 and fig. S4). The percentage increase of associated earthquakes, combined with the rising CEUS earthquake rate, implies that recent seismicity in the CEUS is preferentially occurring near injection wells. The number of nonassociated earthquakes during the same period has also remained stable (Fig. 3). This increase in associated earthquake rate does not correspond to an increase in the rate of wells completed; the well completion rate has remained constant over this period (fig. S5) (26). A portion of the increase in associated earthquakes may be due to increasing spatial coverage of wells, but we suggest that this effect is minimal, considering

that the relative increase in spatial coverage was much more rapid between 1960 and 1980 than in recent years (fig. S5). Wells in central and north-central Oklahoma are the main contributors to the dramatic increase in associated seismicity. New production methods in these regions are generating large volumes of produced water, which are injected at high rates (fig. S6, A and B) (27). Regions such as west Texas, southern Colorado, central Arkansas, and southern Illinois also show concentrations of seismicity associated with injection wells (Fig. 2). However, several regions with large numbers of injection wells appear to be aseismic during the study period, including the Williston Basin of North Dakota (28), the Michigan Basin, and extensive areas of the Texas and Louisiana Gulf Coast (Figs. 1 and 2).

Several operational parameters are hypothesized to influence the likelihood of an induced seismic event: injection rate (19, 24), cumulative injected volume (29, 30), wellhead injection pressure (31), and injection in proximity to crystalline basement (18, 32). Four states—Oklahoma, Arkansas, Colorado, and New Mexico—with both natural and induced earthquakes all have more than 15 years of injection data that include readily ac-

cessible information on monthly injection rate and pressure for a large proportion of operational wells. Using these data, we explore injection operational parameter control on the likelihood that SWD and EOR wells will be associated with earthquakes.

The maximum monthly injection rate of wells across these four states varies by several orders of magnitude, ranging from 100 barrels ( $\sim 15.9 \text{ m}^3$ ) per month (bbl/month) up to 2 million bbl/month ( $\sim 318,000 \text{ m}^3$ ) (Fig. 4A) (33). The average SWD well operates at a mean monthly rate of  $\sim 13,000$  bbl/month. For each histogram bin in Fig. 4, A and B, we calculate the percentage of wells associated with earthquakes. The likelihood that an SWD well is associated with earthquakes increases as the maximum injection rate increases (Fig. 4C). To discern whether the association is random, we estimated upper (95%) and lower (5%) confidence bounds using a bootstrapped resampling method with 10,000 resamples (Fig. 4C) (34, 35). Wells operating at maximum injection rates greater than 300,000 bbl/month fall outside the bootstrap resampling confidence bounds, suggesting a greater-than-expected likelihood of association with an earthquake at a statistical significance near 99%. This is contrasted with wells operating at maximum injection rates less than 100,000 bbl/month, which mostly fall within the bounds of random association. We confirmed this result using spatial distances of association of 5 and 10 km (fig. S7), as well as restricting our well associations to earthquakes greater than  $M \geq 3.0$  (fig. S8). Of the 413 wells operating at injection rates greater than 300,000 bbl/month, 253 (61%) are spatiotemporally associated compared with only 40% of wells operating at injection rates less than 10,000 bbl/month. Additionally, 34 (76%) of the 45 highest-rate SWD wells (injecting more than a million barrels per month) are associated with an earthquake. When SWD operations are examined state by state, the overall percentage associated varies, but the trend of increased earthquake association at higher rates is generally preserved (fig. S9A). Fewer data are available for EOR wells, but we do not observe a clear trend of increasing earthquake association with increasing injection rate for EOR wells (fig. S10A). Without considering geologic or hydrogeologic setting, the highest-rate SWD wells are nearly twice as likely to be near an earthquake as are low-rate SWD wells.

We next examine whether cumulative injected volume affects the likelihood of well association with earthquakes. For the four states examined during the period from 1973 to 2014, cumulative injected volume ranged from 1000 bbl to nearly 100 million bbl (Fig. 4B). Many large cumulative volume wells inject at moderate rates for decades, providing a contrasting data set from maximum injection rate. We do not observe a strong trend of increasing SWD well association as a function of increasing cumulative injected volume (Fig. 4D). The difference between the association rate of wells that have injected more than 1,000,000 bbl cumulatively (45%) and those which

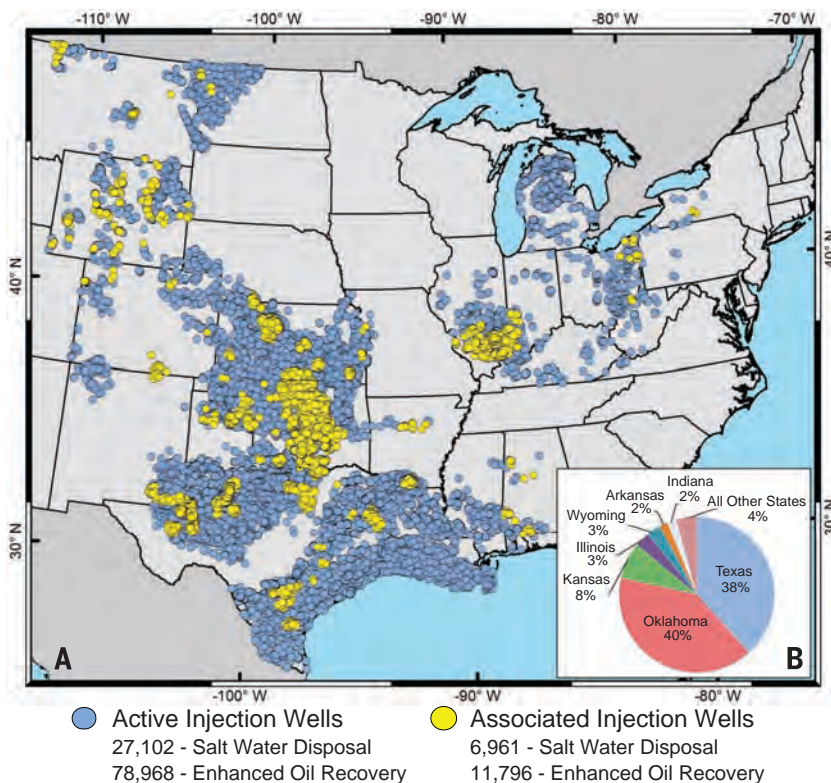


**Fig. 1. Active and associated class II injection wells in the CEUS. (A)** Map showing the location of active class II injection wells in the CEUS. Active injection wells from the database are shown as blue circles. Spatiotemporally associated injection wells, defined as those within a 15-km radius and active at the time of an earthquake, are shown as yellow circles. The CEUS region comprises all states intersected by 109°W longitude and eastward. The total number of wells, including inactive or abandoned wells in the CEUS, is 188,570. Of the 18,757 associated injection wells,  $>77\%$  are currently active. **(B)** The inset pie diagram shows spatiotemporally associated injection wells by state. Only 8% of all injection wells are located in Oklahoma, but 40% of the associated injection wells in the CEUS are located in Oklahoma.



have injected less than 10,000 bbl cumulatively (38%) is not statistically significant, as determined by a bootstrap resampling method (35). The percentage of wells associated with earthquakes at high cumulative injected volumes can be mostly explained by random variation given the total number of associated and nonassociated wells. EOR wells exhibit a trend of earthquake association similar to that of SWD wells as a function of cumulative injected volume (fig. S10B). If we instead calculate cumulative injected volume not for individual wells, but for all wells within 15 km of an associated earthquake, we observe a log-normal distribution of volumes without a clear threshold of increased earthquake association (fig. S11). We do not observe cumulative injected volume as strongly affecting the likelihood of an injection well's association with an earthquake.

The majority of class II injection wells operate at monthly wellhead injection pressures less than 500 pounds per square inch (psi). Reported wellhead pressures for both SWD and EOR wells ranged from 0 to 3000 psi (fig. S12, A and B). In the same four states studied, the proportion of SWD and EOR wells associated with earthquakes show no strong correlation toward increased monthly wellhead pressures (figs. S12 and S13). However, reported monthly wellhead pressure may not always be reliable because many wells report constant wellhead pressures despite changing injection rates. Wellhead injection pressure data may not reflect the pore-pressure conditions in the injection formation due to friction in the wellbore and other factors. In addition, wells reporting zero wellhead pressure still create bottomhole pressure from the hydrostatic fluid column in the well that could be large enough induce an earthquake. There are several hundred wells with zero wellhead pressures that are associated with earthquakes (fig. S12, A and B). This is consistent with field observations of earthquakes induced by wells with zero wellhead pressure (10, 36). We do not consider the reported maximum wellhead pressure to be a controlling factor on injection well and earthquake association. This finding, together with the indication that SWD wells are preferentially associated with earthquakes, underscores the need to collect reservoir pressure data. Ideally, preinjection reservoir pore pressure and bottomhole formation pressure measurements during injection would prove more useful in determining whether a link exists between injection pressure and earthquakes.

Injection depth and proximity to crystalline basement have been hypothesized to affect the likelihood that wells are associated with earthquakes (32). Comparison of injection depths for most states in the CEUS, excluding Mississippi, Indiana, West Virginia, and Alabama, is possible, as these data are more readily available than injection rates and pressures (table S1). Class II injection wells are permitted over a wide range of injection depths from 300 to 4000 m (fig. S14). The majority of both SWD and EOR wells inject between 300 and 1500 m (fig. S14, B and E).

Wells associated with earthquakes also inject over a similarly wide range of injection depths (fig. S14, A and D). We find no clear evidence that increasing injection depth increases the likelihood that a well will be associated with seismicity; the proportion of both SWD and EOR wells associated with earthquakes does not increase with increasing injection depth (fig. S14, C and F).

However, comparison of injection depths neglects the large variations in sediment thickness across the CEUS.

Using a map of sediment thickness across the CEUS (37), we estimate injection proximity to basement for all wells by subtracting injection well depth from the sediment thickness at the closest sediment thickness data point. The

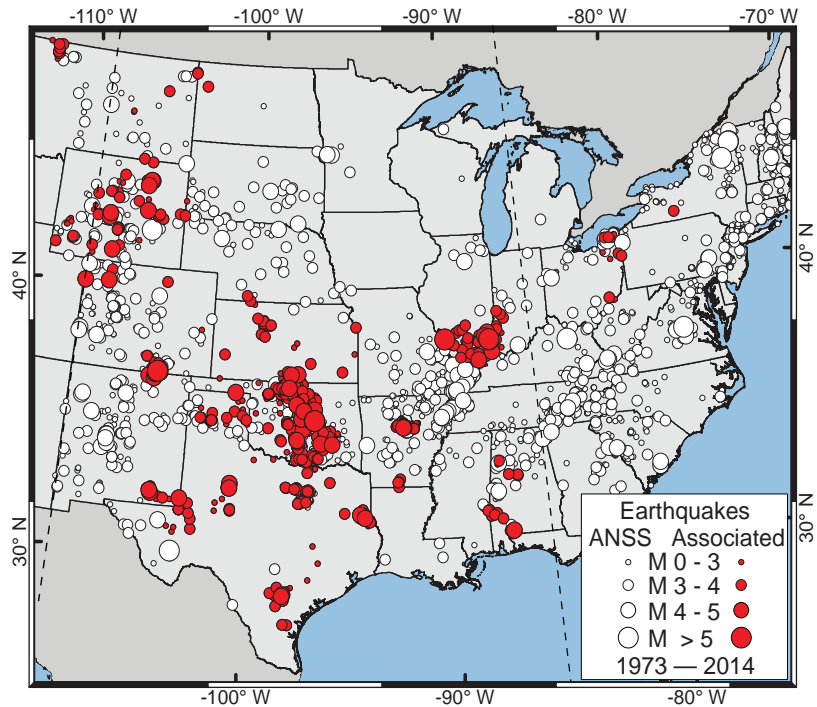
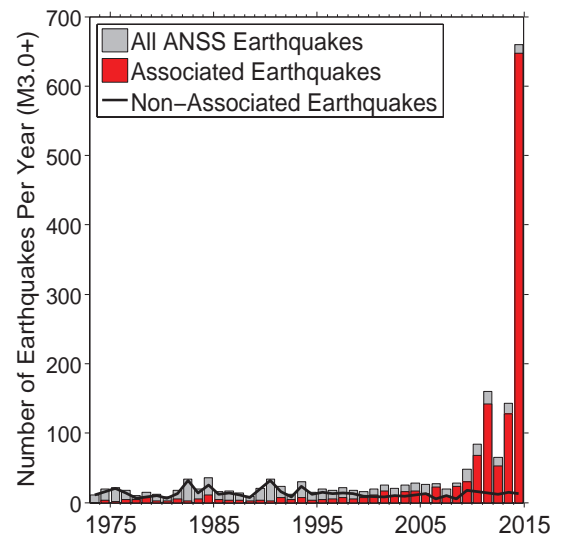


**Fig. 2. Associated earthquakes in the CEUS from 1973 to 2014.** Map showing the locations of  $M \geq 0.0$  earthquakes in the ANSS ComCat earthquake catalog from 1 January 1973 through 31 December 2014. White dots denote earthquakes that are not spatiotemporally associated with injection wells. Red dots denote earthquakes that are spatiotemporally associated with injection wells. Following Ellsworth (7), the U.S. mid-continent is defined by the dashed lines inside of the greater CEUS.

**Fig. 3. Associated and nonassociated earthquakes per year in the U.S. mid-continent.** The gray bars represent the number of  $M \geq 3.0$  earthquakes per year in the U.S. mid-continent (Fig. 2) located by the networks of the ANSS ComCat earthquake catalog from 1 January 1973 to 31 December 2014. The red bars represent the number of earthquakes that are spatiotemporally associated with injection wells. The black line denotes the number of nonassociated earthquakes per year. Over the time period of the catalog, the number of nonassociated earthquakes per year has stayed roughly constant at 10 to 25 per year. Meanwhile, the number of associated earthquakes per year has risen from ~1 to 7 per year in the 1970s to 75 to 190 per year between 2011 and 2013 and >650 earthquakes in 2014.



sediment thickness map was tested against known reference depths of crystalline basement and found to have errors in thickness up to ±15% (table S3). Thousands of wells in the CEUS inject fluid within 500 m of crystalline basement rock, but only a small proportion are associated with seismicity. When taking into account the error in basement depth over the CEUS region, we did not observe a significant correlation between a well's injecting near basement and earthquakes using a bootstrap resampling method (fig. S15). However, injection wells operating very far from basement, between 7 and 12 km vertically, exhibited an association rate near zero. We found similar results for both depth parameters using only well associations with earthquakes greater than *M* 3.0 (figs. S16 and S17). This finding supports the notion that detailed stratigraphic knowledge surrounding the injection interval is necessary to quantify the mechanistic linkage between injection and seismicity (32).

The lack of spatiotemporal association between injection and seismicity in several regions highlights the apparent influence of factors other

than injection well operation. The San Juan Basin of New Mexico, the Williston Basin of North Dakota, the Michigan Basin, and extensive areas of the Texas and Louisiana Gulf Coast contain thousands of SWD and EOR wells that are not associated with seismicity (Fig. 1). In some of these regions, wells inject at rates similar to those in areas such as central Oklahoma, where large numbers of wells are associated with earthquakes. In the aseismic Michigan Basin, 30 wells operate at maximum injection rates greater than 200,000 bbl/month (fig. S18). Obviously, other factors in addition to high injection rate must play a role; the regional state of stress, fault size, fault orientation, the presence of fluid pathways between the injection point and faults, as well as other geologic factors must be examined to assess the potential for injection-induced seismicity (4).

Our analysis shows that injection rate is the most important well operational parameter affecting the likelihood of an induced seismic event in regions and basins potentially prone to induced seismicity. High-rate SWD wells are nearly twice as likely as low-rate wells to be near an earthquake. These high-rate wells perturb the

ambient reservoir pressure by a larger magnitude and over a larger area than low-rate wells, thus increasing the likelihood that pressure changes will reach an optimally oriented, critically stressed fault. Previous studies have shown that high-rate wells exert greater influence on the extent and magnitude of reservoir and fault pressure perturbation (24). At the scale of our study, no other operational parameter was found to have a strong influence on the likelihood of association with an earthquake. The important distinction between operational parameters such as injection rate and cumulative injected volume shows the effect of the recent rise of new production methods and high-rate SWD wells. Thus, the oil and gas industry and regulatory bodies can use this operational parameter to lower the likelihood of earthquakes associated with injection wells.

**REFERENCES AND NOTES**

1. D. M. Evans, *Mt. Geol.* **3**, 23–26 (1966).
2. J. H. Healy, W. W. Rubey, D. T. Griggs, C. B. Raleigh, *Science* **161**, 1301–1310 (1968).
3. C. B. Raleigh, J. H. Healy, J. D. Bredehoeft, *Science* **191**, 1230–1237 (1976).
4. National Research Council, *Induced Seismicity Potential in Energy Technologies* (National Academies Press, Washington, DC, 2013).
5. R. B. Herrmann, S. K. Park, C. Y. Wang, *Bull. Seismol. Soc. Am.* **71**, 731–745 (1981).
6. M. D. Petersen et al., Documentation for the 2008 update of the United States National Seismic Hazard Maps. *U.S. Geol. Surv. Open-File Rep.* **08-1128** (2008).
7. W. L. Ellsworth, *Science* **341**, 1225942 (2013).
8. K. M. Keranen, H. M. Savage, G. A. Abers, E. S. Cochran, *Geology* **41**, 699–702 (2013).
9. A. L. Llenos, A. J. Michael, *Bull. Seismol. Soc. Am.* **103**, 2850–2861 (2013).
10. J. L. Rubinstein, W. L. Ellsworth, A. McGarr, H. Benz, *Bull. Seismol. Soc. Am.* **104**, 2162 (2014).
11. C. Frohlich et al., *J. Geophys. Res.* **119**, 581–593 (2014).
12. S. Horton, *Seismol. Res. Lett.* **83**, 250–260 (2012).
13. M. D. Petersen et al., Incorporating induced seismicity in the 2014 United States National Seismic Hazard Model—Results of 2014 workshop and sensitivity studies. *U.S. Geol. Surv. Open-File Rep.* **2015-1070** (2015).
14. P. A. Hsieh, J. D. Bredehoeft, *J. Geophys. Res.* **86** (B2), 903–920 (1981).
15. C. Nicholson, E. Roeloffs, R. L. Wesson, *Bull. Seismol. Soc. Am.* **78**, 188–217 (1988).
16. J. Ake, K. Mahrer, D. O'Connell, L. Block, *Bull. Seismol. Soc. Am.* **95**, 664–683 (2005).
17. C. Frohlich, C. Hayward, B. Stump, E. Potter, *Bull. Seismol. Soc. Am.* **101**, 327–340 (2011).
18. W.-Y. Kim, W.-Y. Kim, *J. Geophys. Res.* **118**, 3506–3518 (2013).
19. C. Frohlich, *Proc. Natl. Acad. Sci. U.S.A.* **109**, 13934–13938 (2012).
20. U.S. Environmental Protection Agency, Evaluation of impacts to underground sources of drinking water by hydraulic fracturing of coalbed methane reservoirs. EPA Publication 816-F-04-017 (2004).
21. ANSS Comprehensive Catalog (ComCat), U.S. Geological Survey, <http://earthquake.usgs.gov/earthquakes/search/>; accessed 15 February 2015.
22. S. D. Davis, C. Frohlich, *Seismol. Res. Lett.* **64**, 207–224 (1993).
23. A. Frankel, *Seismol. Res. Lett.* **66**, 8–21 (1995).
24. K. M. Keranen, M. Weingarten, G. A. Abers, B. A. Bekins, S. Ge, *Science* **345**, 448–451 (2014).
25. Well shut-in occurs when injection operations are either temporarily or permanently ceased, but the tubing and casing of the well remain in place for possible future reactivation of injection operations.

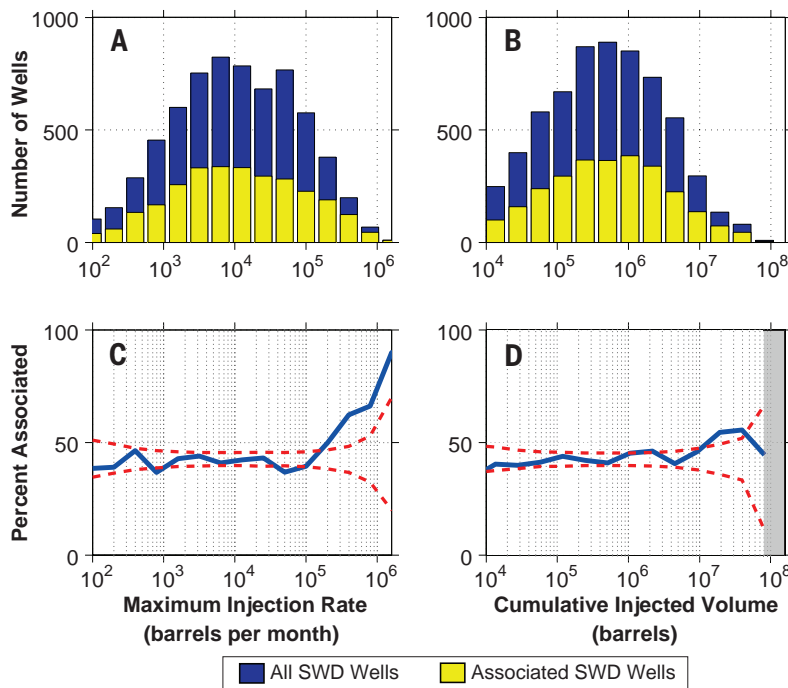


**Fig. 4. Well operational parameter analysis.** (A) Histogram showing the maximum monthly injection rate of salt water disposal (SWD) wells in Oklahoma, Arkansas, Colorado, and New Mexico. The blue and yellow bars show the number of wells operating at a given maximum monthly injection rate for all SWD wells (blue) and SWD wells spatiotemporally associated with an earthquake (yellow). (B) Histogram showing the cumulative injected volume at all wells in the same states as those in (A). The blue and yellow bars represent the number of wells operating at a given cumulative injected volume for all SWD wells (blue) spatiotemporally associated SWD wells (yellow). Injection data for Oklahoma were available from 1995 to 2013, for Arkansas from 1999 to 2013, for Colorado from 1999 to 2014, and for New Mexico from 1994 to 2014. (C and D) The percentage of all wells that are associated with an earthquake in each histogram bin is plotted as a function of (C) maximum monthly injection rate and (D) cumulative injected volume. The two dashed red lines represent the upper (95%) and lower (5%) confidence bounds in each bin generated by 10,000 bootstrap resamples and following the assumption that the rate of association is random. The shaded gray region of (D) indicates a lack of associated wells at the given volume. These data are also broken down state by state and for EOR wells in figs. S9 and S10.

26. Well completion is the process to ready for injection. This process includes installing tubing used to inject fluid, perforating the portion of the well in the injection zone, and casing the well to ensure no injection fluids leakage.
27. K. E. Murray, A. A. Holland, *Shale Shaker* **65**, 98–106 (2014).
28. C. Frohlich, J. I. Walter, J. F. W. Gale, *Seismol. Res. Lett.* **86** (2A), 492–499 (2015).
29. A. McGarr, *J. Geophys. Res.* **81**, 1487–1494 (1976).
30. A. McGarr, *J. Geophys. Res.* **119**, 1008–1019 (2014).
31. L. V. Block, C. K. Wood, W. L. Yeck, V. M. King, *Seismol. Res. Lett.* **85**, 609–624 (2014).
32. Y. Zhang *et al.*, *Ground Water* **51**, 525–538 (2013).
33. The volume conversion from the oil industry standard of barrels to the metric standard of meters cubed is

~6.29 barrels per meter cubed, assuming a 42-gallon oil barrel.

34. B. Efron, R. J. Tibshirani, *An Introduction to the Bootstrap* (CRC press, Boca Raton, FL, 1994).
35. Information on materials and methods is available on *Science Online*.
36. J. Rutqvist *et al.*, *Math. Geosci.* **47**, 3–29 (2015).
37. W. D. Mooney, M. K. Kaban, *J. Geophys. Res.* **115**, B12424 (2010).

#### ACKNOWLEDGMENTS

This work was conducted as a part of the Understanding Fluid Injection Induced Seismicity Project supported by the John Wesley Powell Center for Analysis and Synthesis, funded by the U.S. Geological Survey (grant G13AC00023). We thank J. Hardebeck and W. Ellsworth for their thoughtful comments. This project was aided by injection data

contributed by A. Holland (OK), C. Eisenger (CO), T. Kropatsch (WY), J. Amrhein (IN), T. Tomastik (OH), S. Platt (PA), I. Allred (UT), M. Berry (UT), A. Wickert (TX), and I. Van-Floten (CEUS). This project used earthquake data from the ANSS Comprehensive Catalog. The well data used in this study are available as supplementary materials on *Science Online*.

#### SUPPLEMENTARY MATERIALS

www.sciencemag.org/content/348/6241/1336/suppl/DC1  
Materials and Methods  
Figs. S1 to S18  
Tables S1 to S4  
References (38–46)

16 March 2015; accepted 28 May 2015  
10.1126/science.aab1345

## POLARON DYNAMICS

# Long-lived photoinduced polaron formation in conjugated polyelectrolyte-fullerene assemblies

Rachel C. Huber,<sup>1\*</sup> Amy S. Ferreira,<sup>1\*</sup> Robert Thompson,<sup>1</sup> Daniel Kilbride,<sup>1</sup> Nicholas S. Knutson,<sup>1</sup> Lekshmi Sudha Devi,<sup>1</sup> Daniel B. Toso,<sup>2</sup> J. Reddy Challa,<sup>1</sup> Z. Hong Zhou,<sup>2,3</sup> Yves Rubin,<sup>1†</sup> Benjamin J. Schwartz,<sup>1,3†</sup> Sarah H. Tolbert<sup>1,3,4†</sup>

The efficiency of biological photosynthesis results from the exquisite organization of photoactive elements that promote rapid movement of charge carriers out of a critical recombination range. If synthetic organic photovoltaic materials could mimic this assembly, charge separation and collection could be markedly enhanced. We show that micelle-forming cationic semiconducting polymers can coassemble in water with cationic fullerene derivatives to create photoinduced electron-transfer cascades that lead to exceptionally long-lived polarons. The stability of the polarons depends on the organization of the polymer-fullerene assembly. Properly designed assemblies can produce separated polaronic charges that are stable for days or weeks in aqueous solution.

In biological photosynthetic systems, energy cascade structures promote the spatial separation of photogenerated charges created at the reaction center, preventing their recombination. These energy cascade structures require close proximity of the electron donors and acceptors, on the scale of ~1 nm, and the corresponding electron transfer (ET) processes take only a few picoseconds (7). Similarly, photoexcitation in artificial organic photovoltaic (OPV) cells generates dissociated charges at a donor-acceptor interface on subpicosecond time scales. However, OPVs suffer a large degree of recom-

bination because they rely on phase separation of the conjugated polymer donor and fullerene acceptor into domains on the length scale of 10 to 20 nm to facilitate efficient exciton diffusion and charge transfer (2, 3). The high charge densities present in OPVs, coupled with the low dielectric constant of organic materials, favor carrier recombination before the charges can be extracted through external electrodes. If OPVs could be designed to use ET cascade structures that are reminiscent of photosynthetic complexes, it should be possible to greatly improve charge separation and reduce recombination losses (4).

Here we describe how molecular self-assembly can enable dissolved OPV materials (conjugated polymers and fullerenes) in aqueous solution to mimic the ET cascade structures of biological complexes and allow us to “spatially” control photogenerated charges. We demonstrate efficient long-time charge separation following photoexcitation: The ET cascade produces separated polarons that are exceptionally stable for weeks, a lifetime that is unprecedented

for OPV materials. Although long polaron lifetimes have been observed in covalently linked donor-acceptor dyads and triads (5) and micellar structures (6), our use of standard organic photovoltaic materials sets this work apart. In addition, our use of self-assembly provides potential future advantages in reproducibility and scalability, both of which are major hurdles for conventional OPVs with kinetically controlled structures (7–9). Finally, the photoinduced charge separation we achieve takes place in water, opening possibilities for the “green” production of artificial photosynthetic devices.

The particular materials used in this study are a combination of a conjugated polyelectrolyte, poly(fluorene-alt-thiophene) (PFT) (10), and several regioisomers of the charged fullerene derivatives C<sub>60</sub>-N,N-dimethylpyrrolidinium iodide [C<sub>60</sub>(PI)<sub>n</sub>], where n is the number of charged pyrrolidinium iodide groups (11) (Fig. 1, A to C). PFT is a water-soluble semiconducting polyelectrolyte whose bis-alkylated sp<sup>3</sup>-hybridized fluorenyl carbon forms a wedge-shaped monomer that facilitates the assembly of the charged polymer into rod-like micelles (Fig. 1B); details of how this polymer assembles have been published previously (10). Because of the charged nature of the polymer, the electron acceptor(s) must also carry cationic charges to avoid heterocoagulation. The synthesis of C<sub>60</sub>(PI)<sub>n</sub>, depending on the reaction conditions, produced multiadducts with n ranging from 2 to 5, including multiple regioisomers for each n. To avoid confusion, we will refer to C<sub>60</sub>(PI)<sub>n</sub> with n = 3 to 5 as “higher” adducts and fullerenes with n = 2 as “mixed-bis” adducts.

We achieved control over the solution-phase aggregation of these materials by exploiting the different solubility properties of the conjugated polyelectrolyte and charged fullerene derivatives. Mixed-bis adducts show limited solubility (without PFT) in aqueous solution, whereas higher adducts are water soluble at high concentration. This difference suggests that the mixed-bis adducts should coassemble in aqueous solution with PFT, a result we confirmed by cryogenic electron microscopy (cryoEM), small-angle x-ray scattering (SAXS), and luminescence quenching studies. CryoEM images of pure PFT, PFT:mixed-bis adducts, and PFT:high adducts

<sup>1</sup>Department of Chemistry and Biochemistry, University of California–Los Angeles (UCLA), Los Angeles, CA 90095-1569, USA. <sup>2</sup>Department of Microbiology, Immunology and Molecular Genetics, and the Biomedical Engineering Program, UCLA, Los Angeles, CA 90095, USA. <sup>3</sup>The California NanoSystems Institute (CNSI), UCLA, Los Angeles, CA 90095, USA. <sup>4</sup>Department of Materials Science and Engineering, UCLA, Los Angeles, CA 90095, USA.

\*These authors contributed equally to this work. †Corresponding author. E-mail: tolbert@chem.ucla.edu (S.H.T.), schwartz@chem.ucla.edu (B.J.S.), rubin@chem.ucla.edu (Y.R.)



Supplementary Materials for

**High-rate injection is associated with the increase in U.S. mid-continent seismicity**

M. Weingarten, S. Ge, J. W. Godt, B. A. Bekins, J. L. Rubinstein

correspondence to: [matthew.weingarten@colorado.edu](mailto:matthew.weingarten@colorado.edu)

**This DOC file includes:**

Materials and Methods  
Figs. S1 to S18  
Tables S1 to S4  
References 38-46

## Materials and Methods

### Methods: Injection Data Quality Control

Injection data quality control was applied to the monthly injection rate and monthly injection pressure data for Oklahoma, New Mexico, Colorado and Arkansas. The corrected data were used in the statistical comparison of associated wells by maximum monthly injection rate, cumulative injected volume and injection pressure (**Figs. 4, S7-8**). The most common errors noted in the recorded data were simple keying errors in the entry of the monthly injection rate. Class II disposal wells are typically drilled by the operator and permitted by the state regulatory body with *a priori* knowledge of the expected monthly injection rate in a given area. Therefore, a given well will typically operate at similar rates over its lifetime. If there are changes in injection rate they typically occur gradually over several months to years. To account for keying errors, we expect that when a well is operational (i.e. injection rate > 0 bbl/month) each monthly injection rate should fall within one standard deviation of the expected monthly injection rate. If an observed rate is several standard deviations from the expected monthly rate, the specific monthly injection rate is almost always a keying error in which digits were accidentally added to the value or digits were not entered in the correct order. These errors were present in each state studied and were most often evident in the highest monthly injection rates (i.e. millions of bbl/month). To correct these errors, we calculated a simple percent error for each monthly injection rate in a given well's record:

$$\text{Percent Error} = \frac{Q_{obsij} - Q_{mean}}{Q_{obsij}}$$

where  $Q_{obsij}$  is the observed monthly injection rate at month  $i$  and year  $j$  and  $Q_{mean}$  is the observed mean monthly injection rate over the well's lifetime. Errors greater than +/- 71% were manually reviewed to ensure the given well was not experiencing an uncharacteristic increase or decrease in injection rate for a period of time greater than the month in question. If the reviewed monthly injection rate was considered a keying error, the rate was changed to the mean monthly injection rate of the well's record. Fewer than 1% of all injection rates were changed according to this protocol.

Another source of potential bias are that injection rates less than 500 bbl/month were typically reported in 100 barrel increments (i.e. 100, 200 or 300 bbl/month). This is potentially an operational reporting bias and was not corrected in the dataset.

### Methods: Calculating maximum monthly injection rate & cumulative injected volume

Maximum monthly injection rate and cumulative injected volume were calculated differently depending on whether a given injection well was associated or non-associated with an earthquake. If an injection well was not associated with an earthquake, the maximum monthly injection rate was determined from the maximum rate from the well's entire injection history. Similarly, the cumulative injected volume for non-associated wells was calculated as the sum of the well's entire injection history. However, if the well was associated with an earthquake, the maximum monthly injection rate was determined from only the portion of the injection history prior to the date of the associated earthquake. The cumulative injected volume of associated wells was similarly calculated as the sum of the injection history prior to the date of the associated earthquake. If a well was associated with multiple earthquakes, the most recent earthquake was used as the prior date for calculation of injection metrics.



Calculating the two injection parameters differently depending on a well's association with an earthquake is a function of the potential causal relationship between the given well and earthquake. The spatiotemporal filter identifies wells that are associated with a given earthquake. However, a causal relationship between well operation and earthquake occurrence can be due only to the portion of the injection history prior to the associated earthquake date. Injection after the associated earthquake date can only be causally related to subsequent associated earthquakes. Therefore, the maximum monthly injection rate and cumulative injected volume for associated well's are only calculated for the portion of well's history prior to the associated earthquake (**Fig. 4**).

#### Methods: Bootstrapped resampling to estimate confidence intervals

To assess whether the association between operational parameters and earthquake occurrence is a random process, we estimate confidence intervals for the expected percent of wells associated in any given bin of the respective distributions using a bootstrap resampling method (*Efron and Tibshirani, 1994*).

For each of the bins in the distribution we perform the bootstrap resampling protocol:

- 1.) Create a set of wells equal to all of the wells in the entire distribution.
- 2.) Randomly sample from that set, with replacement, a number of wells equal to the number of wells in the particular bin.
- 3.) Count how many of the random samples in step 2 are associated with earthquakes.
- 4.) Repeat steps 2 & 3 10,000 times.
- 5.) Sort the number of associated counts from smallest to largest.
- 6.) The 500th and 9,500th largest number of counts are the 5% and 95% confidence for that bin.

After the protocol is run for each bin in the histogram distribution we generate a 5% and 95% confidence bound from the 5% and 95% confidence in each bin (**Fig. 4, S7-11**).



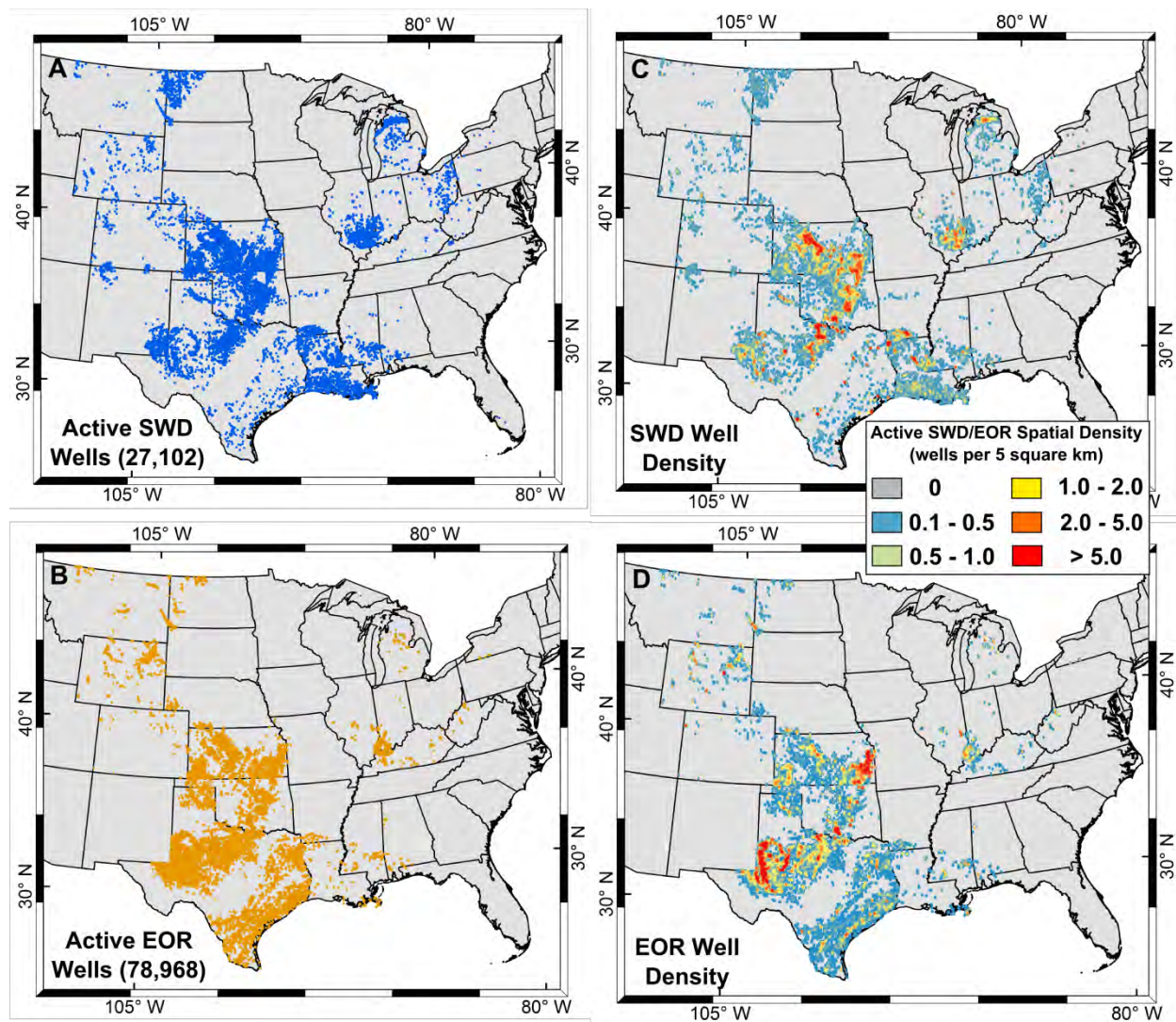


**Figure S1:** Maps of (A) active salt water disposal (SWD) wells, (B) active enhanced oil recovery wells (EOR) wells, (C) the number of active SWD wells per five square kilometers and (D) the number of EOR wells per five square kilometers. EOR wells are spatially dense in the Permian Basin and Fort Worth Basin in Texas, the Ardmore Basin of south-central Oklahoma, and the southern Fort City Basin of southeastern Kansas. SWD wells are spatially dense in the Fort Worth Basin in Texas and from central Oklahoma northwards into central Kansas.

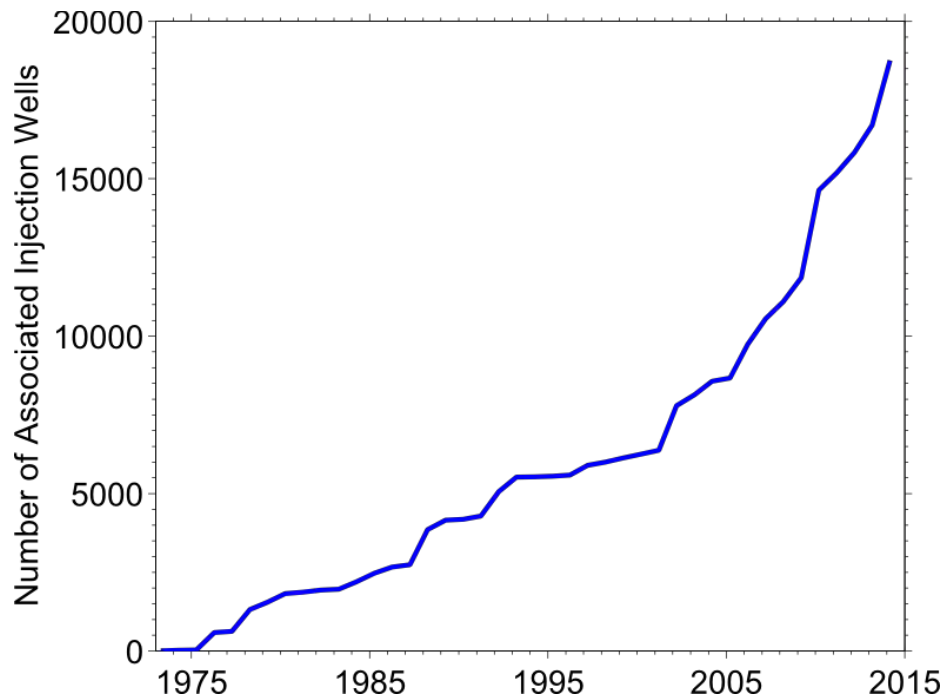


**Figure S2:** The number of associated injection wells through time identified using a spatial filter of 15 km combined with a temporal filter for active wells only. For each associated well, we find the date of the first associated earthquake. We then count the cumulative number of associated wells prior to the given year to produce the curve. We observe an increase in the number of associated wells through time; 6,129 wells were associated with earthquakes in the year 2000. By the end of 2014, the number of associated wells has tripled to more than 18,757.

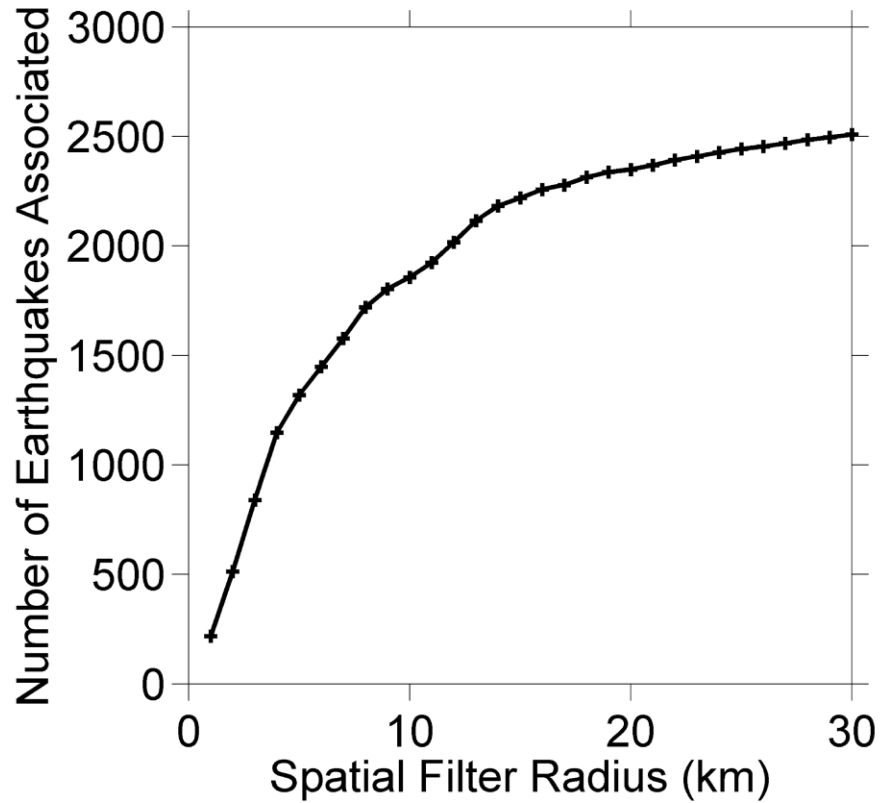


**Figure S3:** The number of associated earthquakes as a function of spatial filter radius using the Advanced National Seismic System's (ANSS) earthquake catalog from 1973 - March 24, 2014. The number of associated earthquakes is not linearly related to spatial filter radius. Similar numbers of earthquakes are associated using spatial filters of 15 km or 30 km. This is an unexpected result, as one might expect the rate of associated earthquakes to increase with increasing spatial distance. The number of earthquakes associated with a 15 km filter is 2,219 whereas a 30 km filter associates 2,510 earthquakes. Thus, the lower sensitivity of earthquake association to spatial filter radius past 15 km indicates this radius is appropriate for spatial filtering.

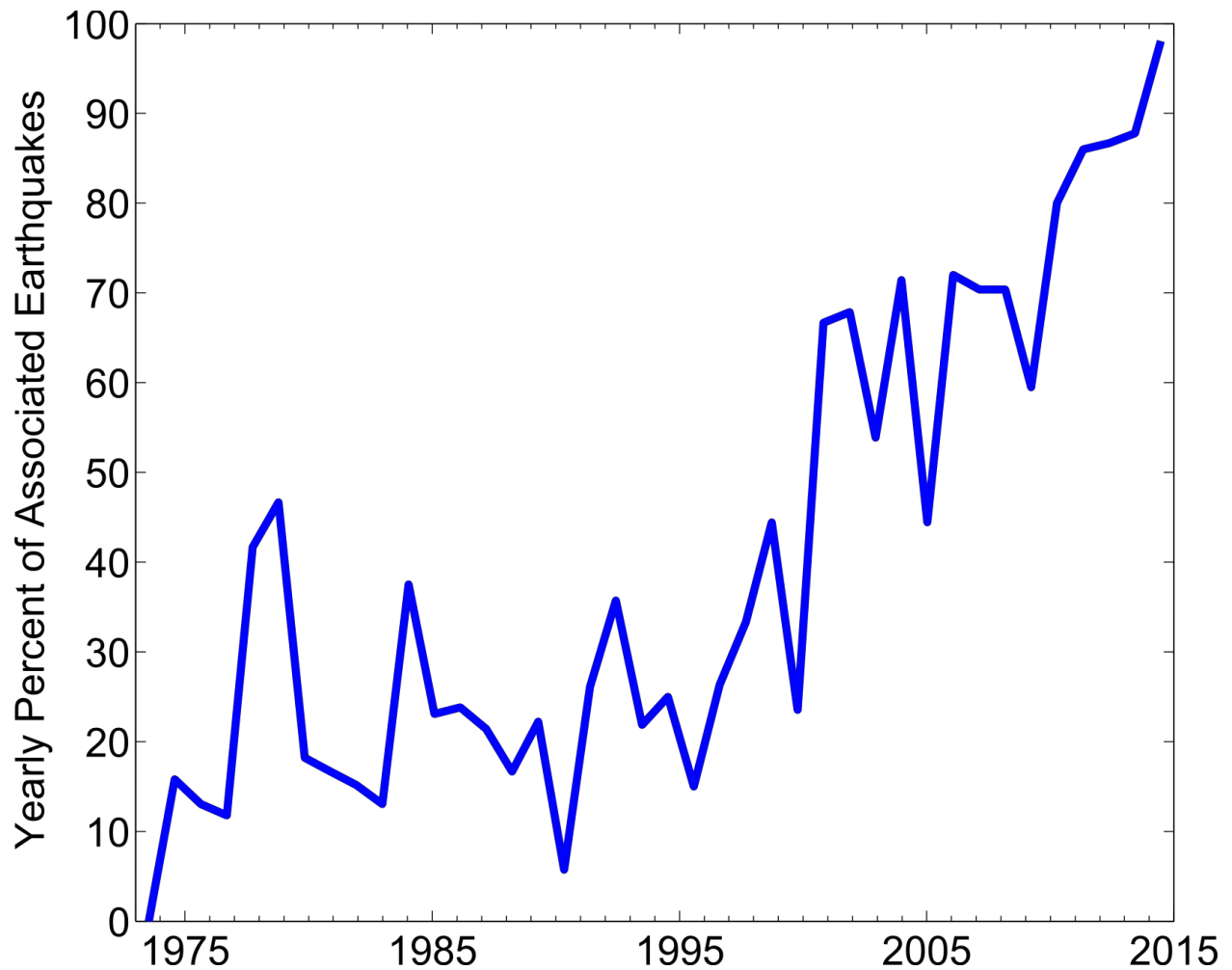


**Figure S4:** The curve shows the yearly percent of central and eastern U.S. (CEUS) earthquakes ( $M \geq 3.0$ ) spatiotemporally associated with injection wells through time. Since 2000, the yearly percent of earthquakes associated with injection wells has risen from an average of 22% from 1973-2000 to over ~98% in 2014. During the same time period, the cumulative percent of all CEUS earthquakes associated with injection wells has increased from 20% from 1973-2000 to 70% in the last 14 years.



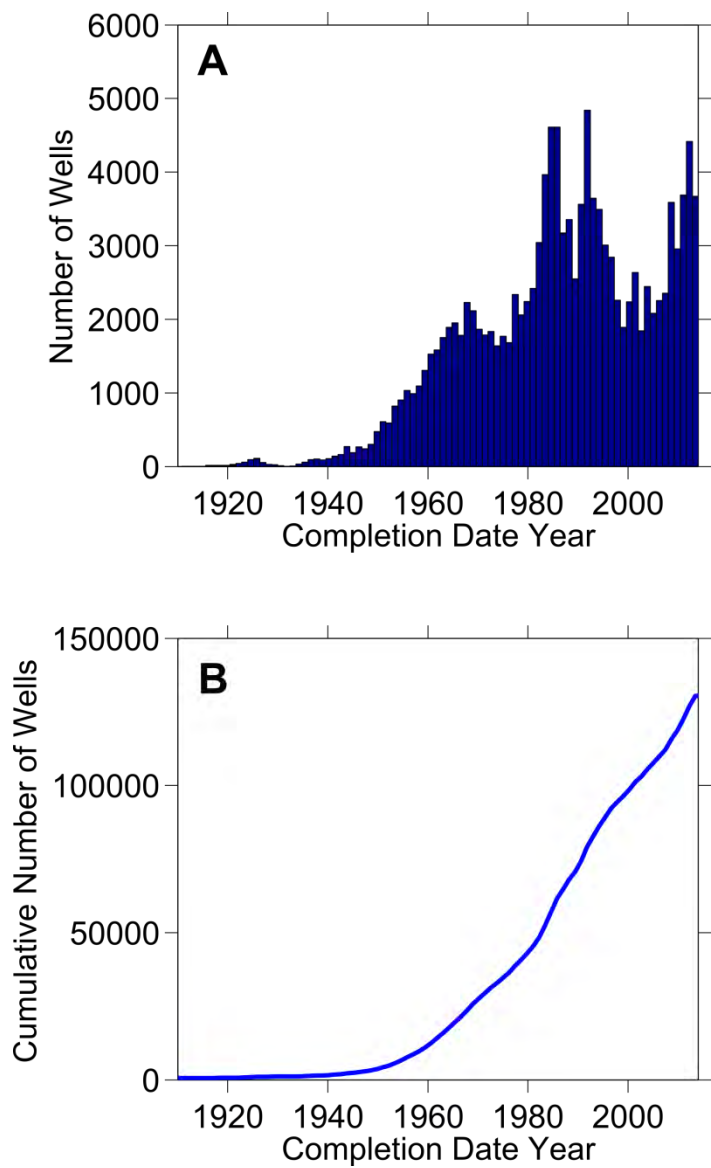


**Figure S5:** A.) A histogram of the number of wells completed in a given year through time. The number of completed Class II injection wells each year varies according to fluctuations in domestic oil and gas operations. B.) A cumulative curve of the number of Class II injection wells completed by a given year. The overall rate of wells completed each year has not markedly changed since the early 1980s.

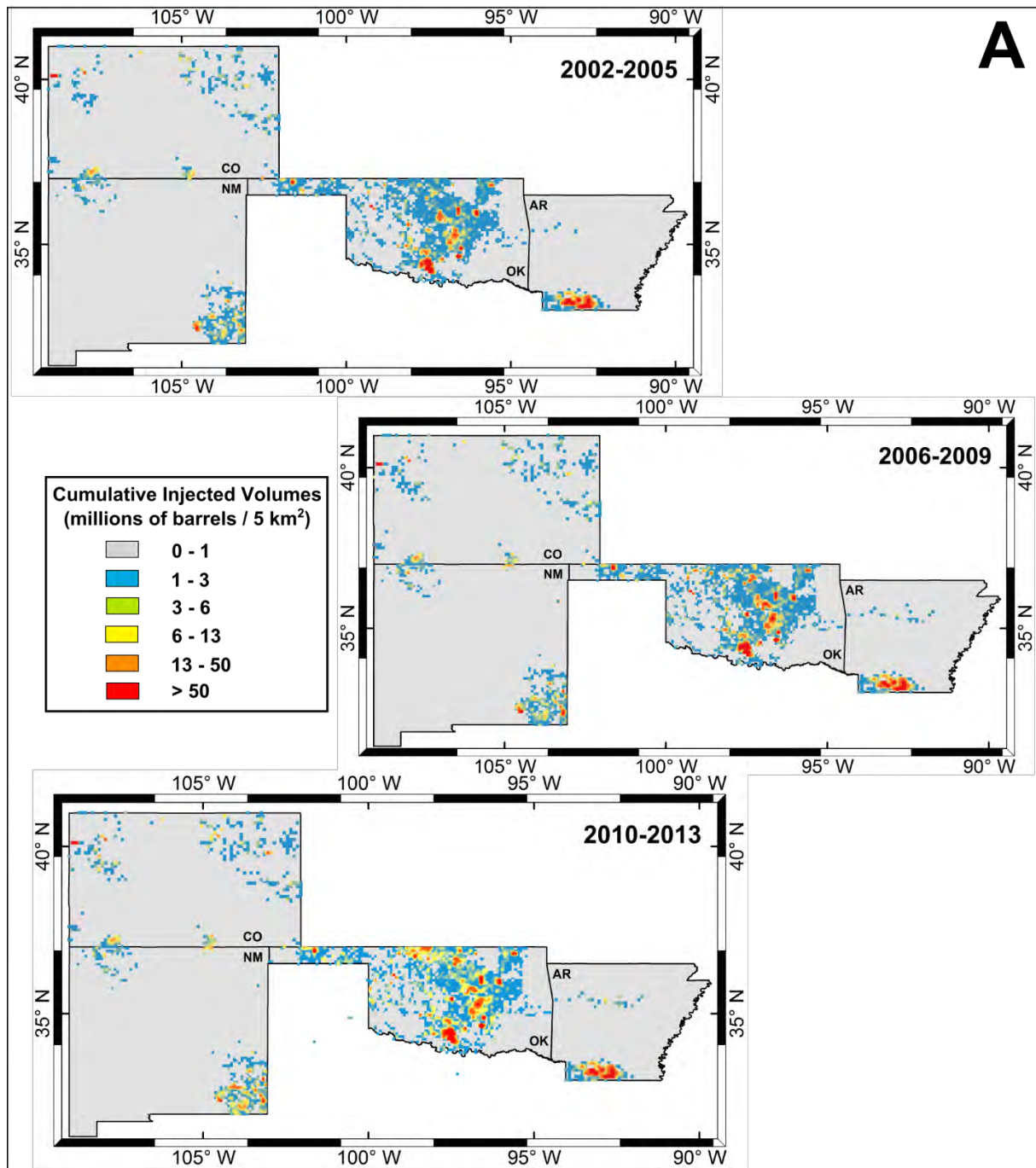


**Figure S6A:** Maps of cumulative injected volume per five square kilometer boxes in Oklahoma (OK), Colorado (CO), New Mexico (NM) and Arkansas (AR) for three time periods: 2002-2005, 2006-2009 and 2010-2013. Each map sums the volume injected over a given time period. Areas of highest cumulative injected volume during these time periods are in southern, central and north-central OK as well as southern AR. Prior to the onset of seismic rate changes in the mid-late 2000s, cumulative injected volumes in several regions in these four states were similar to that of today. However, some regions, such as north-central Oklahoma, have experienced distinct injection increases in the past decade.

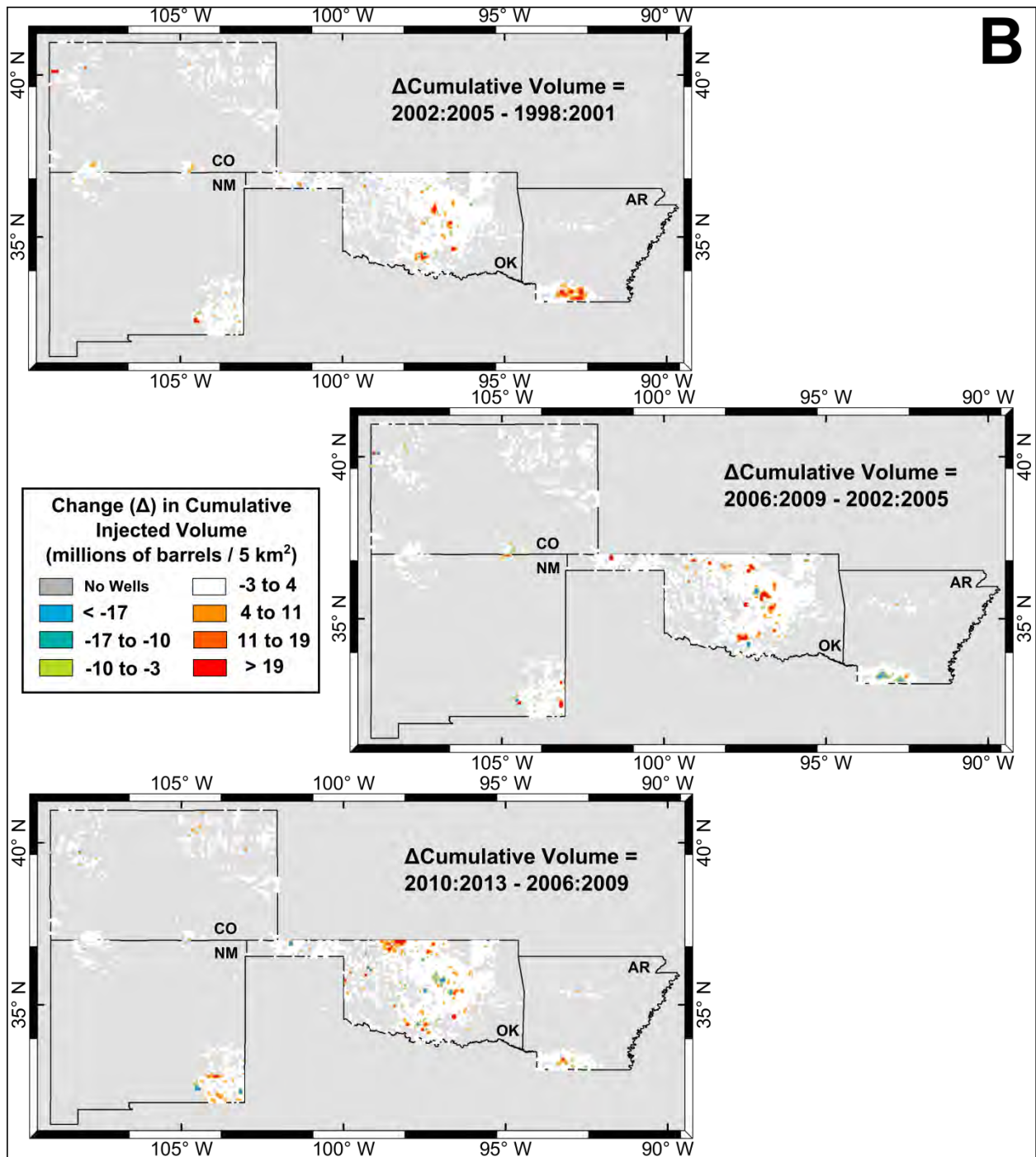


**Figure S6B:** Maps showing the change in cumulative injected volume per five square kilometer boxes relative to four time periods. The upper map differences volumes summed from 2002-2005 from volumes summed from 1998-2001. The middle map differences volumes summed from 2006-2009 from volumes summed from 2002-2005. The lower map differences volumes summed from 2010-2013 from volumes summed from 2006-2009. The middle map shows the activation of injection operations in central Oklahoma between 2006-2009. The bottom map shows the activation of injection operations in north-central Oklahoma between 2010-2013.

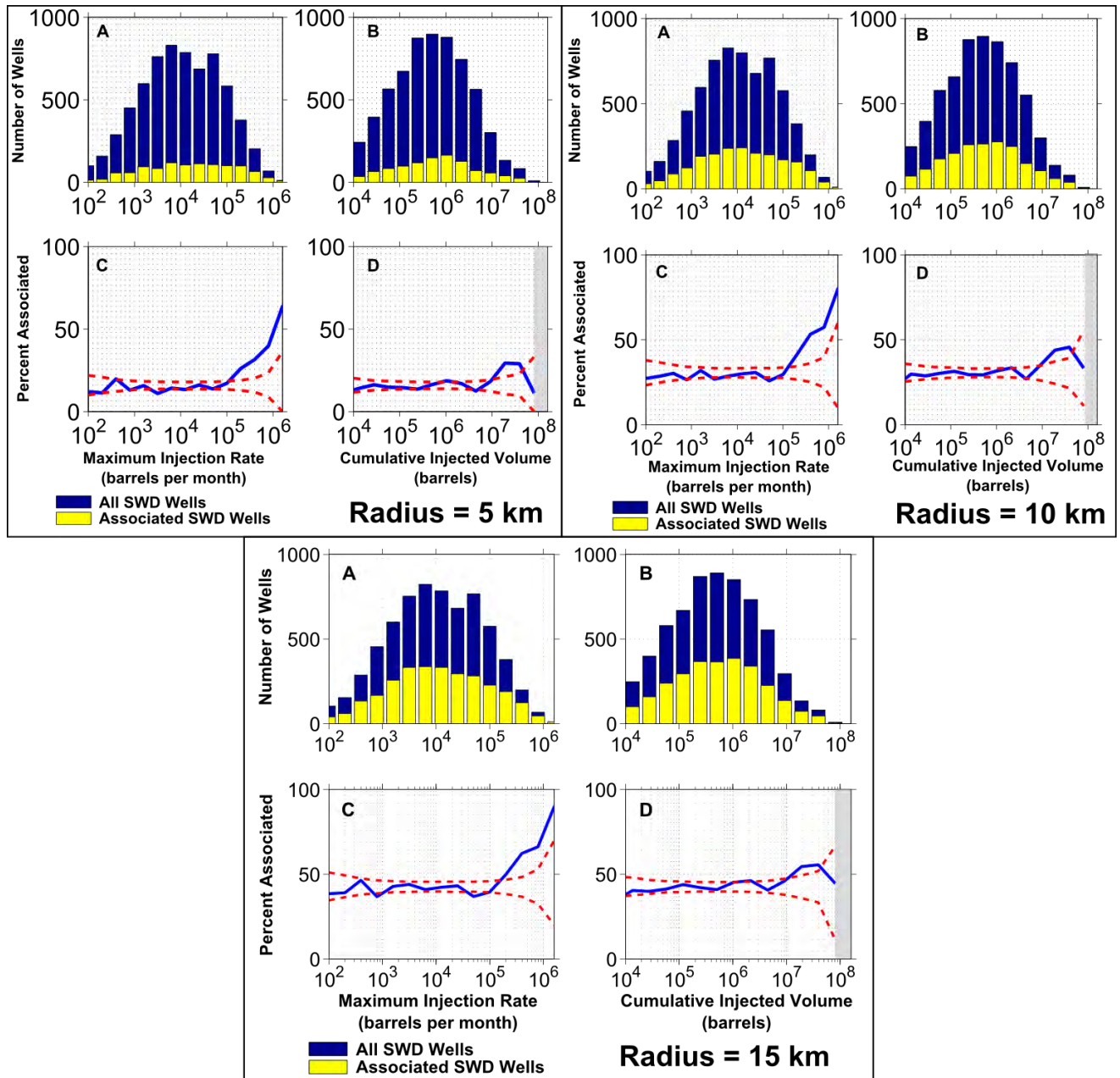


**Figure S7:** Injection parameter analysis for three radii of spatial association: 5 km, 10 km and 15 km. The number of associated wells decreases as a function of decreasing spatial radius as shown in the histograms of associated versus all SWD wells. However, the statistics show high injection rate wells are still preferentially associated with earthquakes using both a 5 km and 10 km radius. In addition, cumulative injected volume does not show a clear trend of increasing association with increasing cumulative injected volume.



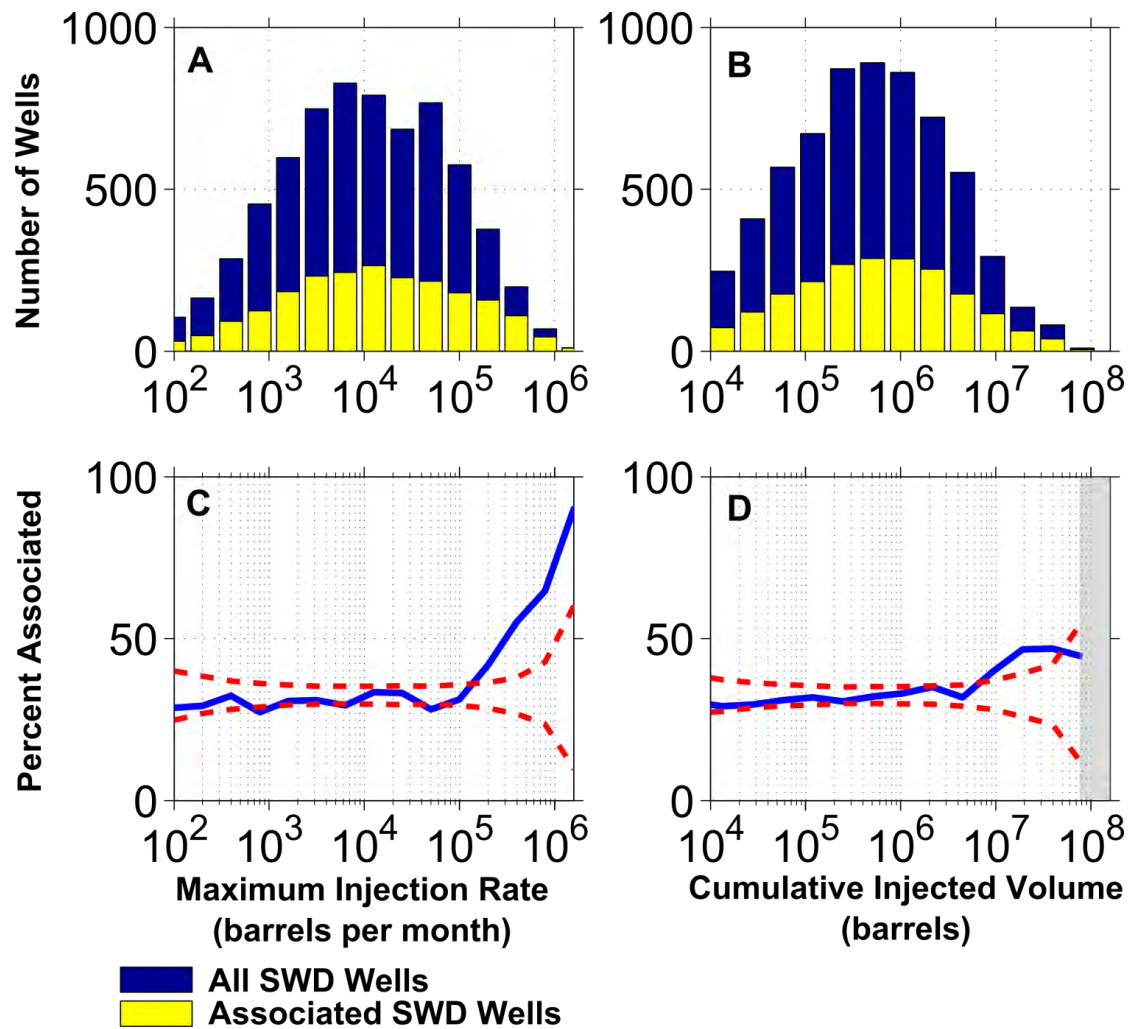


**Figure S8:** We re-ran the same operational parameter analysis from Figure 4 (maximum injection rate and cumulative injected volume) associating wells with earthquakes only greater than  $M3.0$ . **(A)** Histogram showing the maximum monthly injection rate of salt water disposal (SWD) wells in Oklahoma, Arkansas, Colorado, and New Mexico. The blue bars show the maximum monthly injection rate for all SWD wells, whereas the yellow bars show the maximum monthly injection rate for SWD wells spatiotemporally associated with an earthquake. **(B)** Histogram showing the cumulative injected volume at all wells in the same states as (A). The blue distribution represents the cumulative injection volume for SWD wells, while the yellow distribution is for spatiotemporally associated wells. Injection data for Oklahoma was available from 1995-2013, for Arkansas from 1999-2013, for Colorado from 1999-2014, and for New Mexico from 1994-2014. **(C-D)** The percentage of all wells that are associated with an earthquake in each histogram bin is plotted as a function of (C) maximum monthly injection rate and (D) cumulative injected volume. The two dashed red lines represent the upper (95%) and lower (5%) confidence bounds in each bin generated by 10,000 bootstrap resamples and following the assumption that the rate of association is random. The shaded grey region of (D) indicates non-associated wells at the given volume.

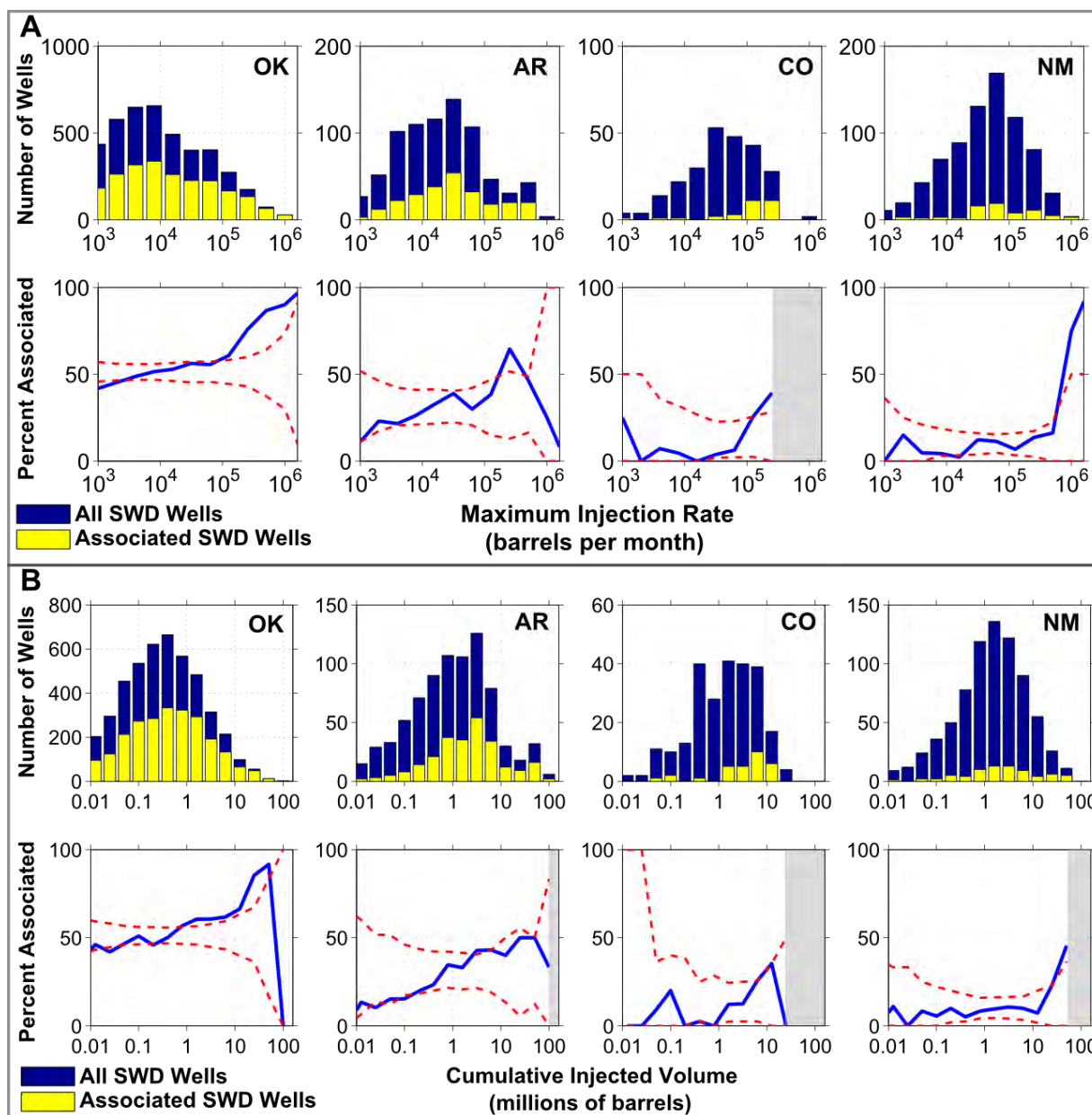


**Figure S9:** (A) Upper row shows histograms of the maximum monthly injection rate of all SWD wells in Oklahoma (OK), Arkansas (AR), Colorado (CO), and New Mexico (NM). The blue bars indicate the maximum monthly injection rate for all salt-water disposal (SWD) wells; yellow bars show the maximum monthly injection rate for wells spatiotemporally associated with an earthquake. The lower row of charts shows the percentage of all wells associated with an earthquake in each histogram bin. The two dashed red lines represent the upper (95%) and lower (5%) confidence bounds in each bin generated by 10,000 bootstrap resamples and following the assumption that the rate of association is random. The shaded regions of the plots denote that no associated maximum monthly injection rate is observed at those values. (B) Histograms of cumulative injected volume for the same wells and states depicted in (A) as well as their respective percent associated plots.

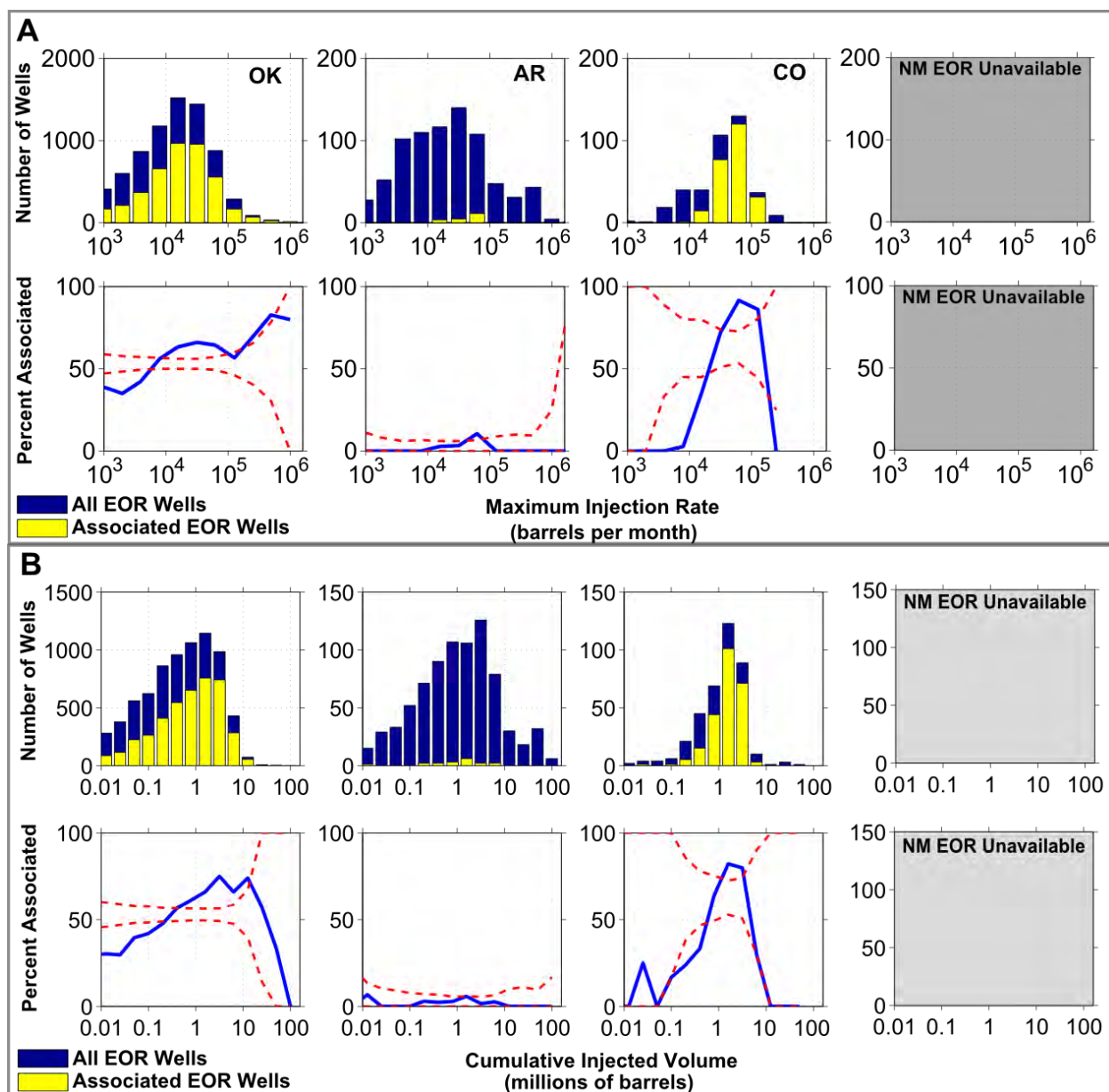


**Figure S10:** (A) Upper row shows histograms of the maximum monthly injection rate of all EOR wells in Oklahoma (OK), Arkansas (AR) and Colorado (CO). No EOR injection data was available for New Mexico (NM). The blue bars indicate the maximum monthly injection rate for all enhanced oil recovery (EOR) wells; yellow bars show the maximum monthly injection rate for wells spatiotemporally associated with an earthquake. The lower row of charts shows the percentage of all wells associated with an earthquake in each histogram bin. The two dashed red lines represent the upper (95%) and lower (5%) confidence bounds in each bin generated by 10,000 bootstrap resamples and following the assumption that the rate of association is random. The shaded regions of the plots denote that no associated maximum monthly injection rate is observed at those values. (B) Histograms of cumulative injected volume for the same wells and states depicted in (A) as well as their respective percent associated plots.

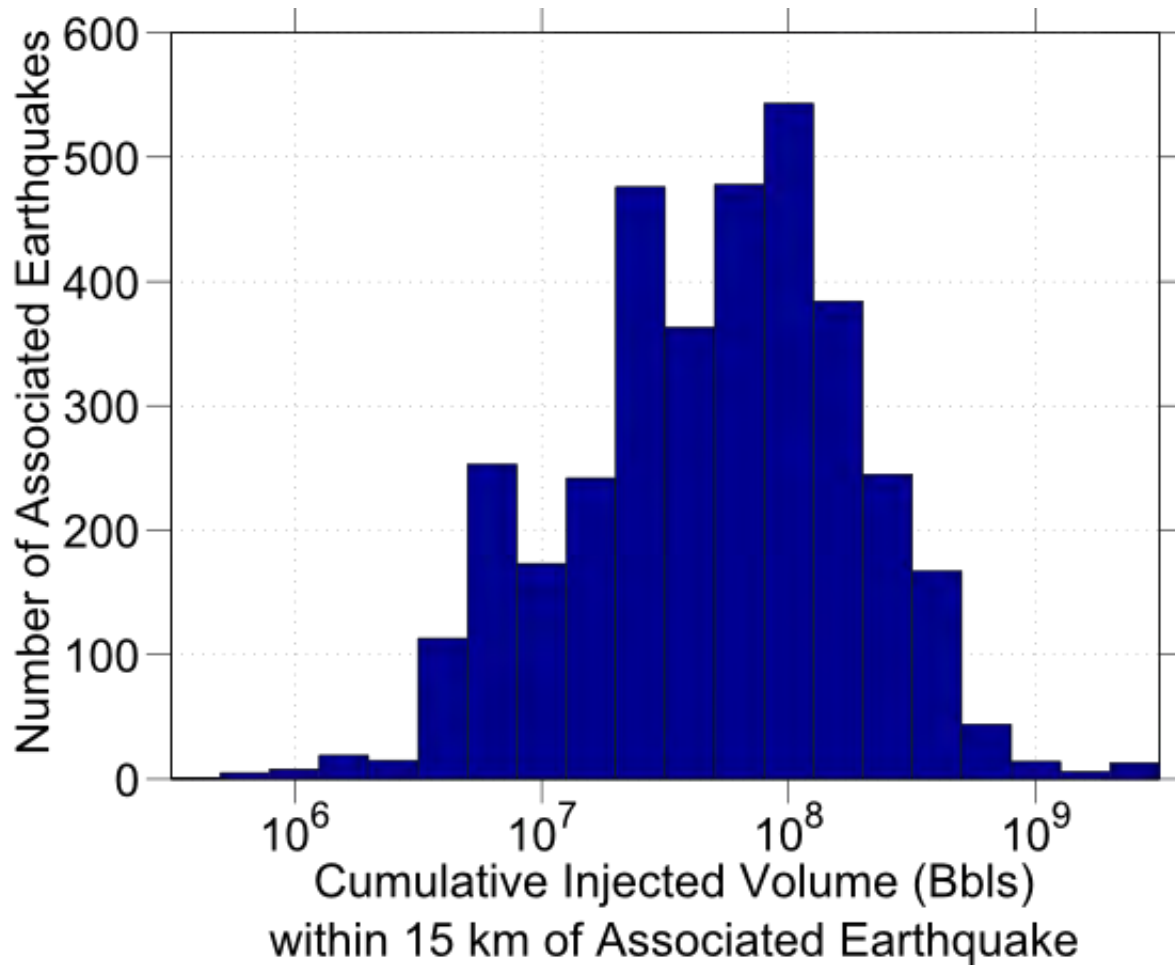


**Figure S11:** Histogram of cumulative injected volume within 15 km of each associated earthquake. While all associated earthquakes have some amount of volume injected within 15 km, we observe a log-normal distribution of the number of associated earthquakes at a given injected volume. Our interpretation of the data suggests the level of injected volume within 15 km of associated earthquakes does not correlate to the number of associated earthquakes observed.



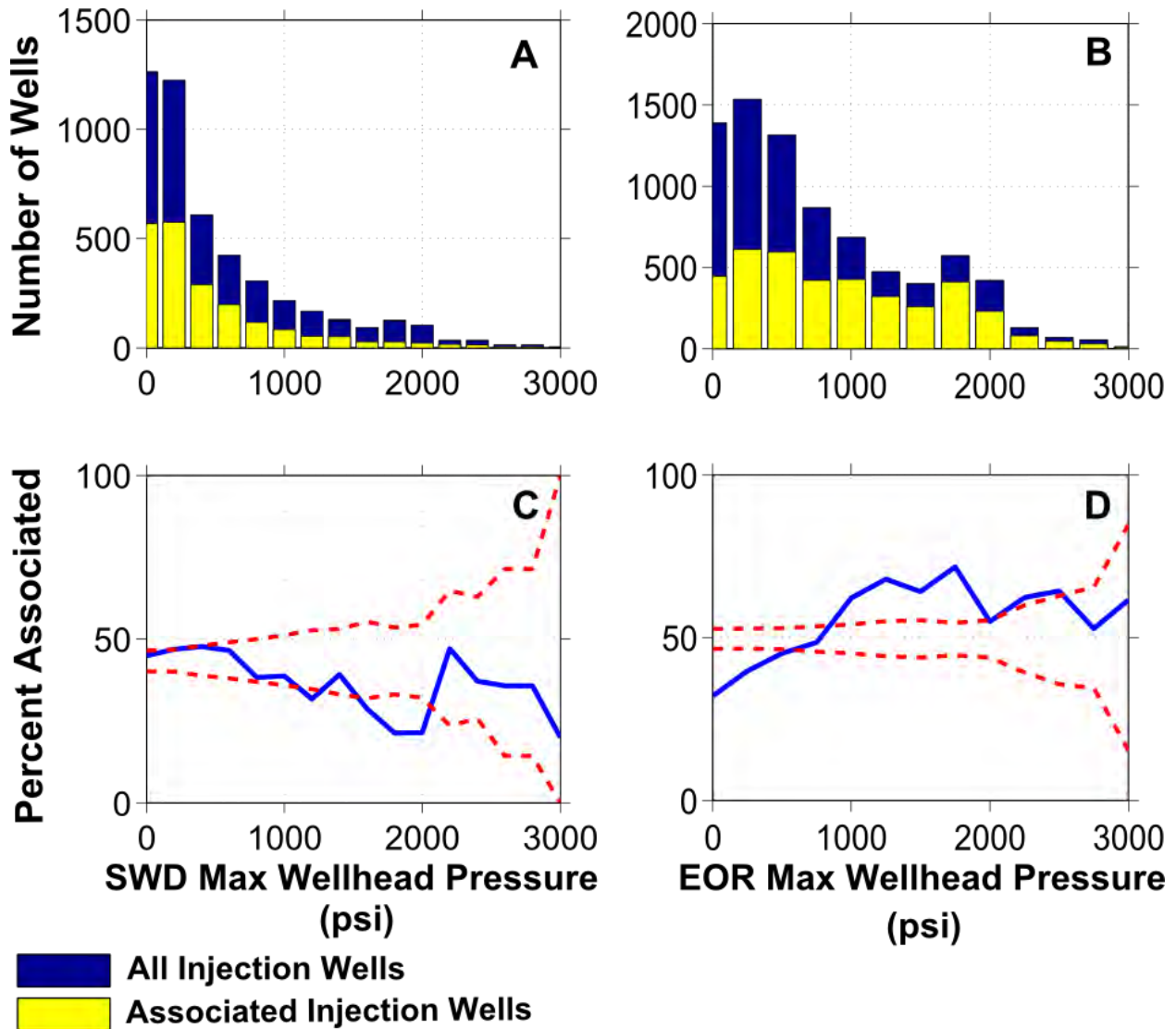


**Figure S12:** (A) Histogram of maximum wellhead pressure for salt water disposal wells (SWD) and associated SWD wells (yellow) for Oklahoma, New Mexico, Arkansas and Colorado combined. (B) Histogram of maximum wellhead pressure for enhanced oil recovery wells (EOR) and associated EOR wells in Oklahoma, Arkansas and Colorado combined. (C-D) The percent of wells associated with an earthquake in each histogram bin at a given maximum wellhead pressure for (C) SWD wells and (D) EOR wells. The dashed red lines are the upper (95%) and lower (5%) confidence intervals in each bin generated by 10,000 bootstrap resamples and following the assumption that the rate of association is random. No clear trend of increasing wellhead pressure for associated wells is evident for either SWD wells or EOR wells.

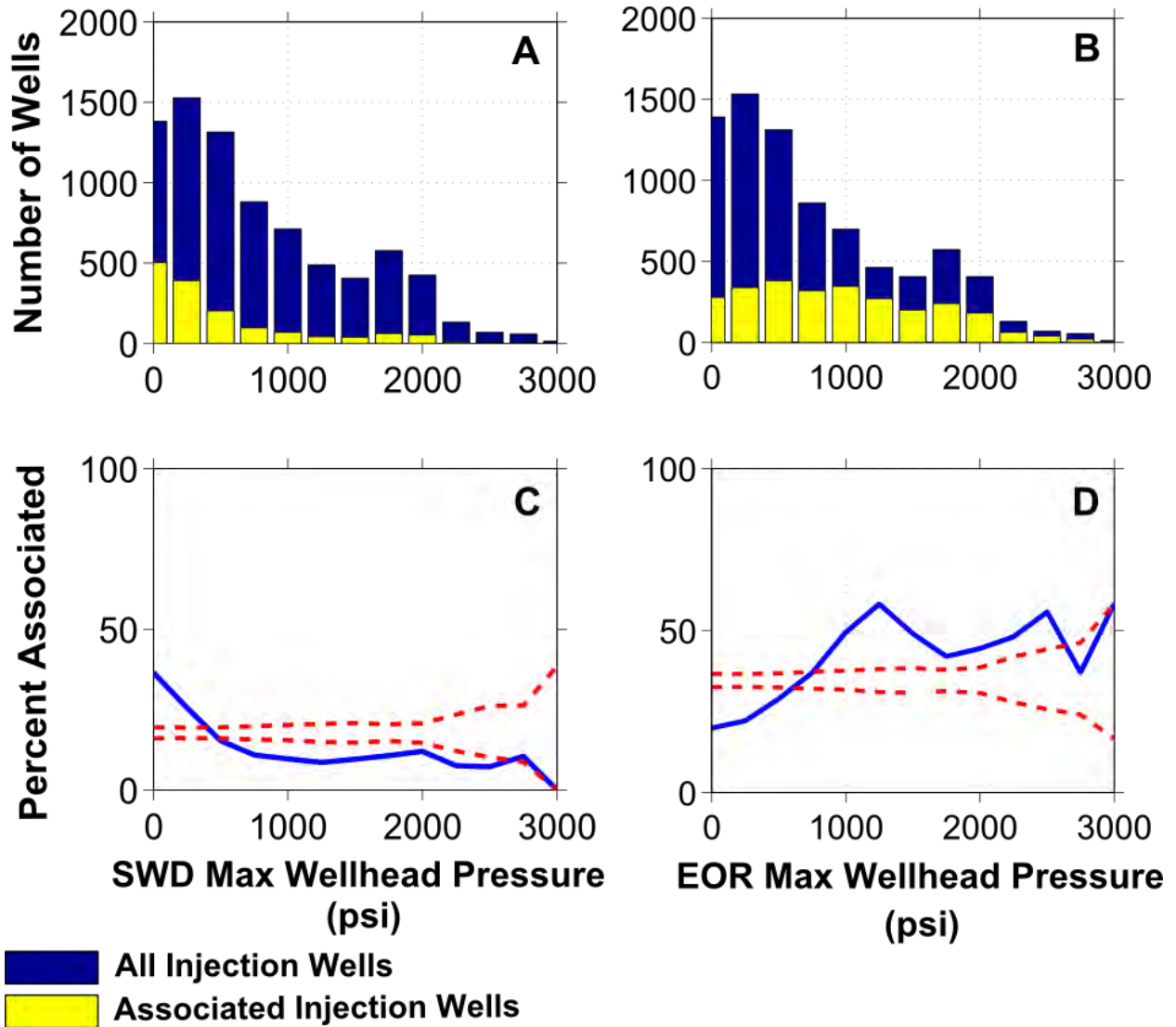


**Figure S13:** Injection pressure analysis for wells associated with earthquakes greater than M3.0 (A) Histogram of maximum wellhead pressure for salt water disposal wells (SWD) and associated SWD wells (yellow) for Oklahoma, New Mexico, Arkansas and Colorado combined. (B) Histogram of maximum wellhead pressure for enhanced oil recovery wells (EOR) and associated EOR wells in Oklahoma, Arkansas and Colorado combined. (C-D) The percent of wells associated with an earthquake in each histogram bin at a given maximum wellhead pressure for (C) SWD wells and (D) EOR wells. The dashed red lines are the upper (95%) and lower (5%) confidence intervals in each bin generated by 10,000 bootstrap resamples and following the assumption that the rate of association is random. No clear trend of increasing wellhead pressure for associated wells is evident for either SWD wells or EOR wells.

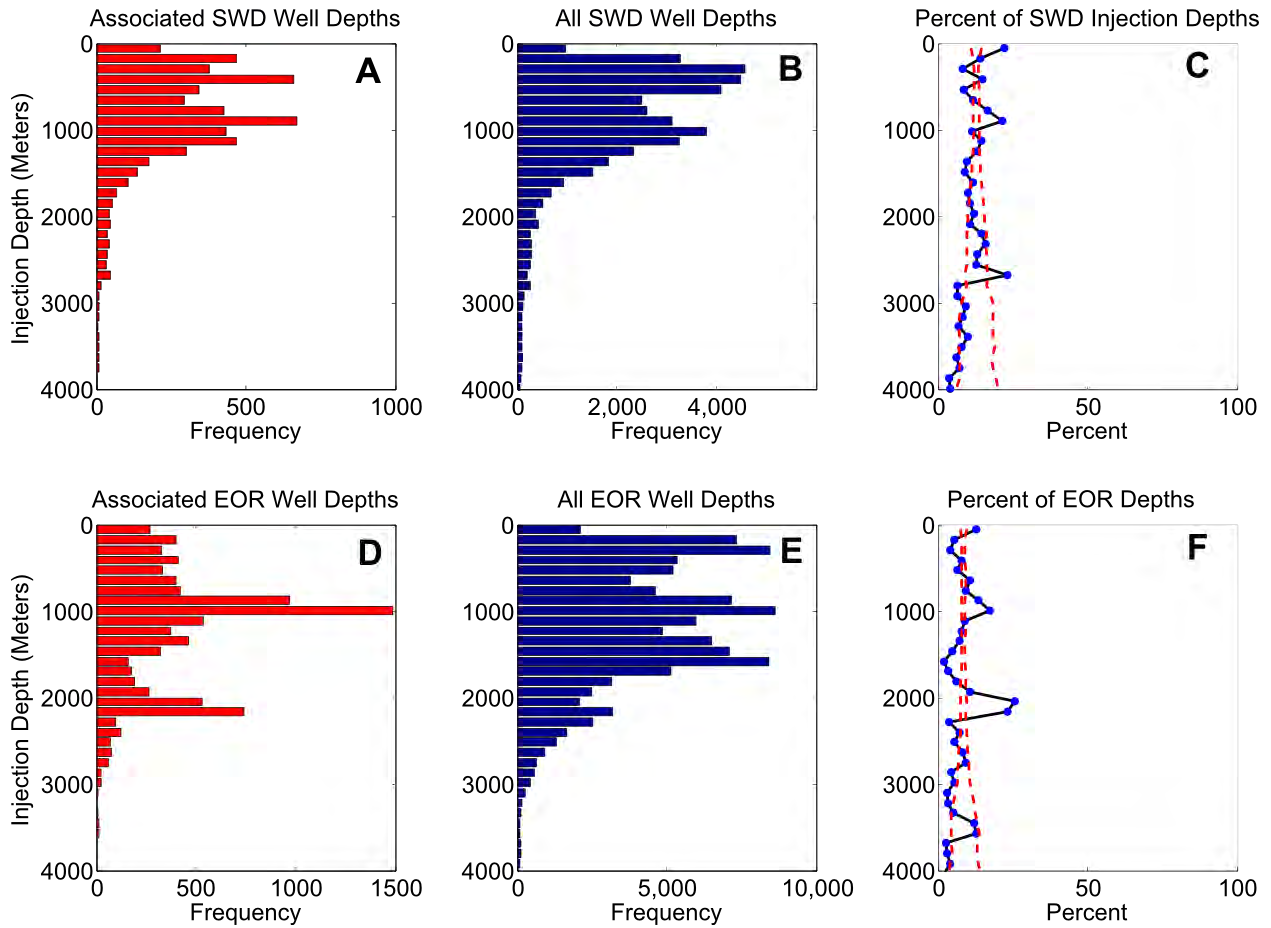


**Figure S14:** Histograms of injection depths for (A) associated salt-water disposal (SWD) wells and (B) all SWD wells. (C) The percent of SWD wells associated with seismicity for each injection depth bin. Histograms of injection depths for (D) associated enhanced oil recovery (EOR) wells and (E) all EOR wells. (F) The percent of EOR wells associated with seismicity for each injection depth bin. The dashed red lines in C and F represent the 5% and 95% confidence intervals generated by 10,000 bootstrap resamples. No clear trend of increasing depth correlating to increased numbers of associated wells is evident.

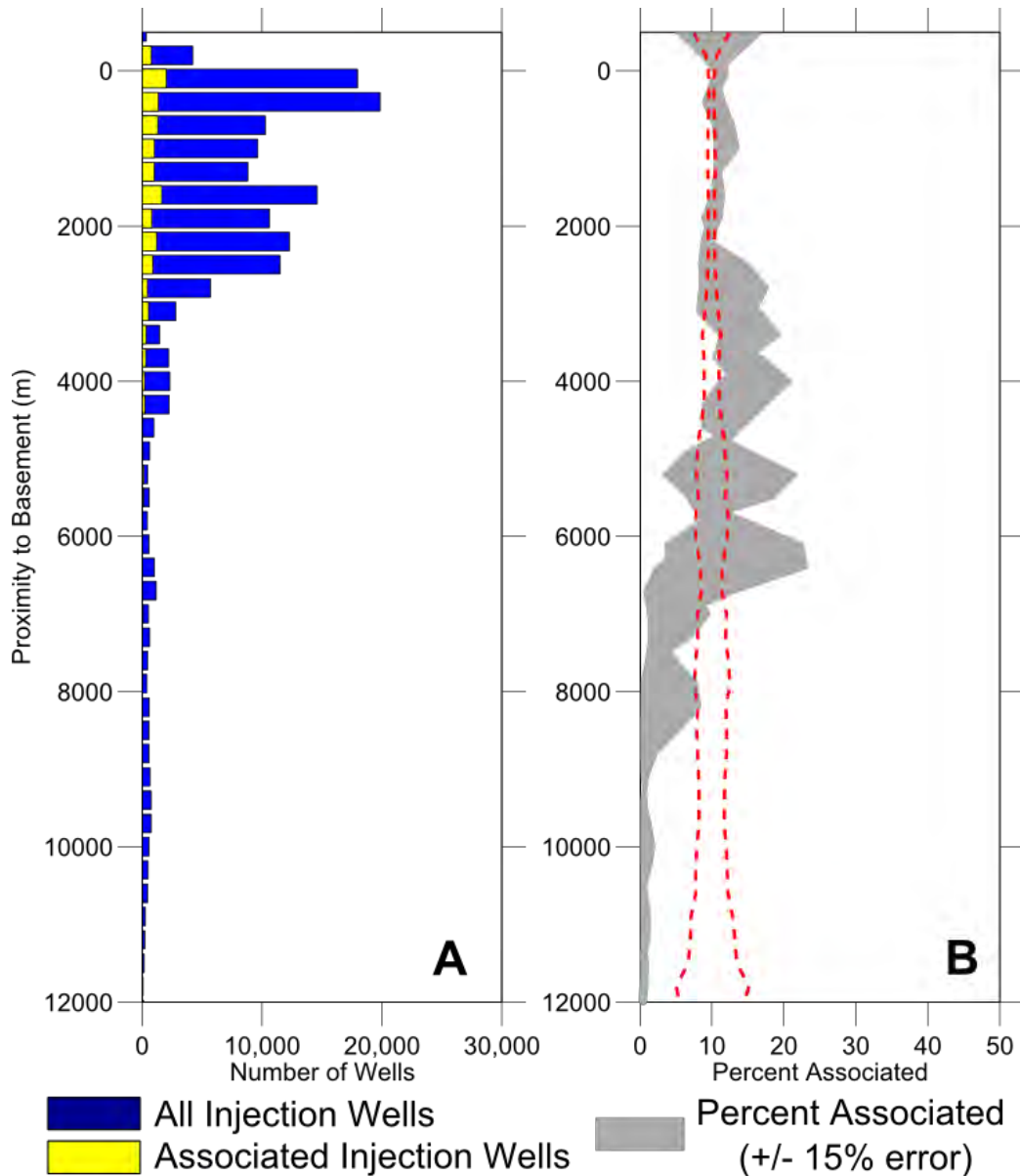


**Figure S15:** Injection well depths plotted by each well's proximity to crystalline basement rock. (A) Proximity to basement for associated wells (yellow bars) versus all wells (blue bars) and (B) percent of all wells associated with earthquakes at a given proximity to basement (shaded grey region) with a plus or minus 15 percent error in the basement depth included. The dashed red lines represent the 5% and 95% confidence intervals generated by 10,000 bootstrap resamples. Increasing positive values indicate increasing distance between a given injection well's depth and the depth of crystalline basement rock. We do not identify any correlation between the proximity of injection to basement and association rate. However, well's injecting between 7 - 12 kilometers from crystalline basement exhibiting a near-zero association rate.

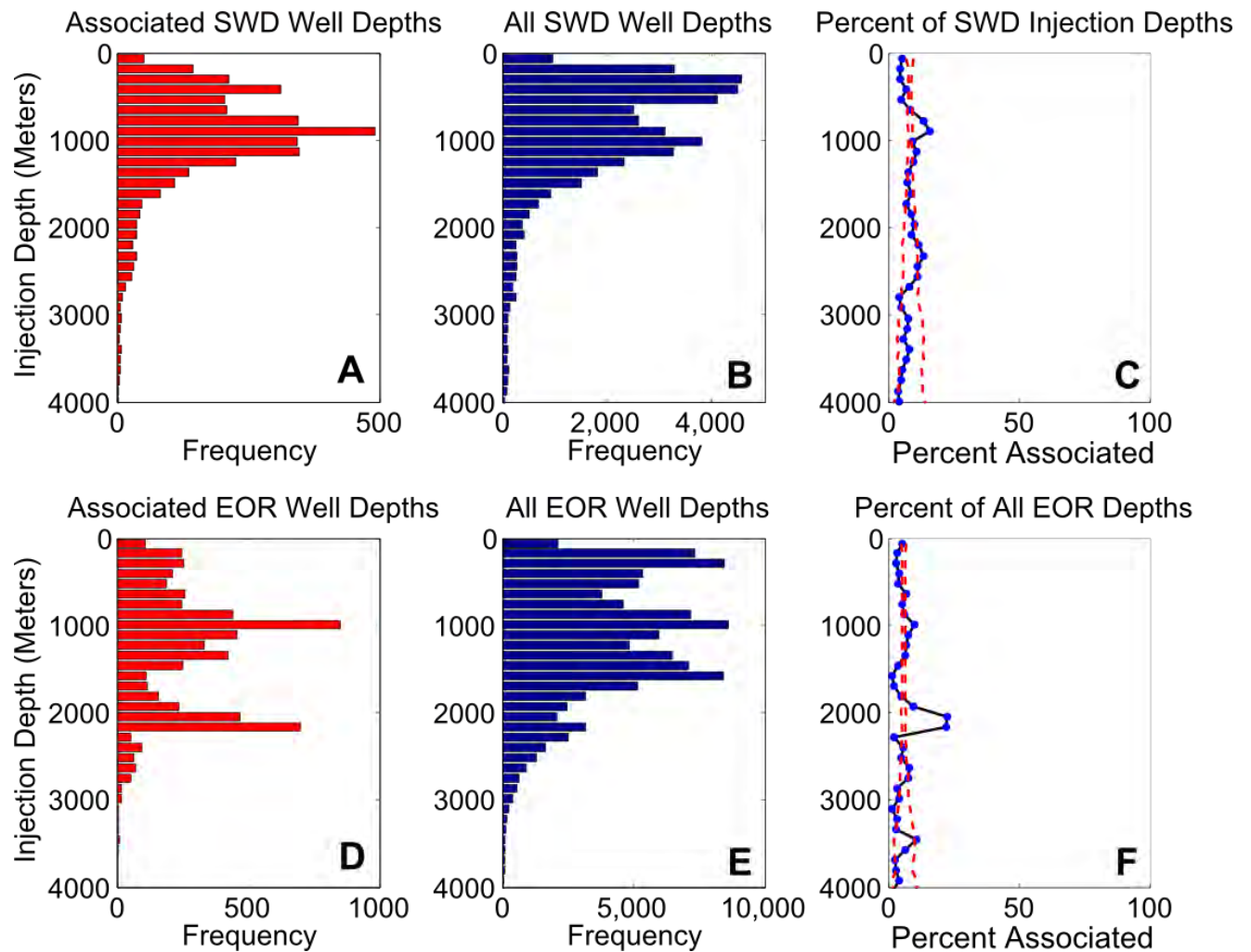


**Figure S16:** Histograms of injection depths for (A) associated salt-water disposal (SWD) wells and (B) all SWD wells. (C) The percent of SWD wells associated with seismicity for each injection depth bin. Histograms of injection depths for (D) associated enhanced oil recovery (EOR) wells and (E) all EOR wells. (F) The percent of EOR wells associated with seismicity for each injection depth bin. Spatiotemporal filtering analysis was re-run using only earthquakes greater than  $M3.0$  to see the effect of injection depth on large magnitude earthquakes. The dashed red lines in C and F represent the 5% and 95% confidence intervals generated by 10,000 bootstrap resamples. No clear trend of increasing depth correlating to increased numbers of associated wells is evident.



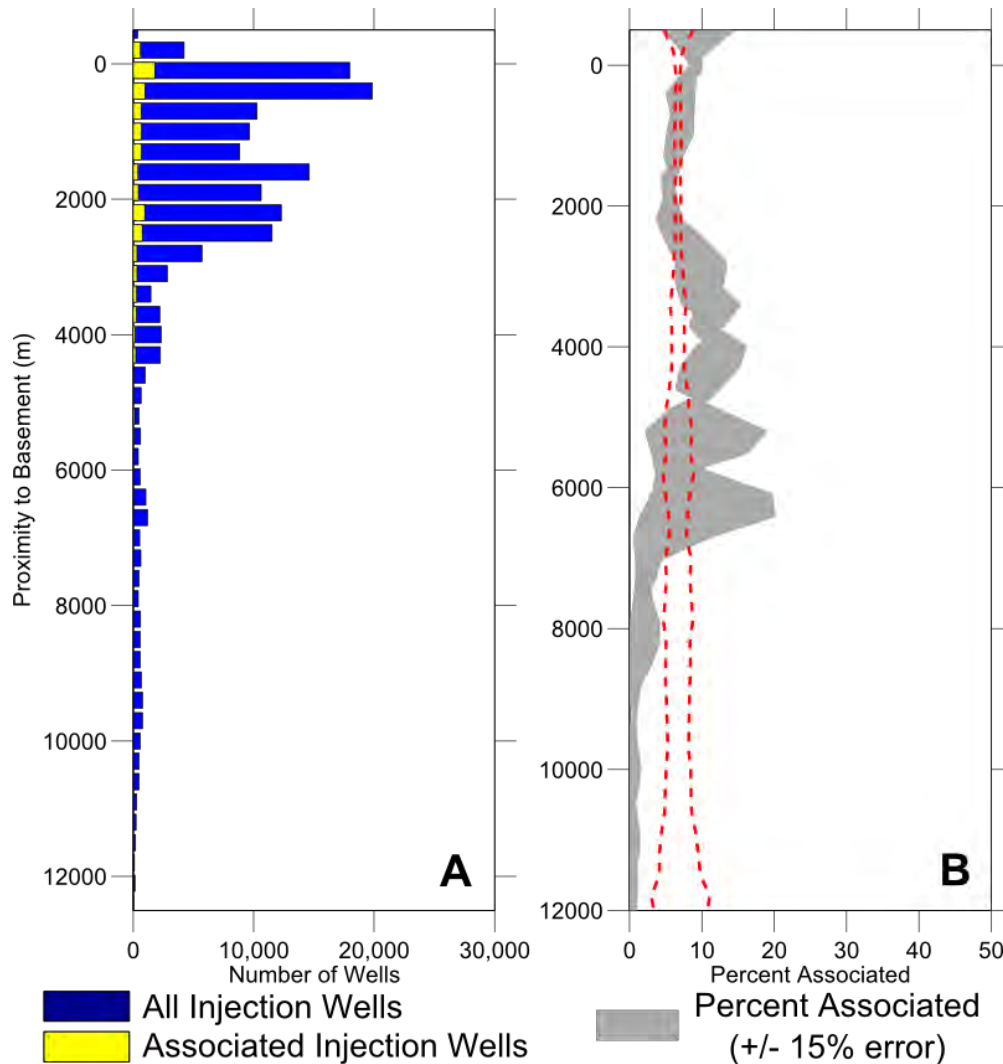


**Figure S17:** Injection well depths plotted by each well's proximity to crystalline basement rock. In this analysis, we used a spatiotemporal filter which only associates earthquakes greater than  $M3.0$  to see the effect of proximity to basement on larger magnitude earthquakes. (A) Proximity to basement for associated wells (yellow bars) versus all wells (blue bars) and (B) percent of all wells associated with earthquakes at a given proximity to basement (shaded grey region) with a plus or minus 15 percent error in the basement depth included. The dashed red lines represent the 5% and 95% confidence intervals generated by 10,000 bootstrap resamples. Increasing positive values indicate increasing distance between a given injection well's depth and the depth of crystalline basement rock. We do not identify a strong correlation between the proximity of injection to basement and association rate. However, well's injecting between 7 and 12 kilometers from basement exhibit a near-zero association rate.

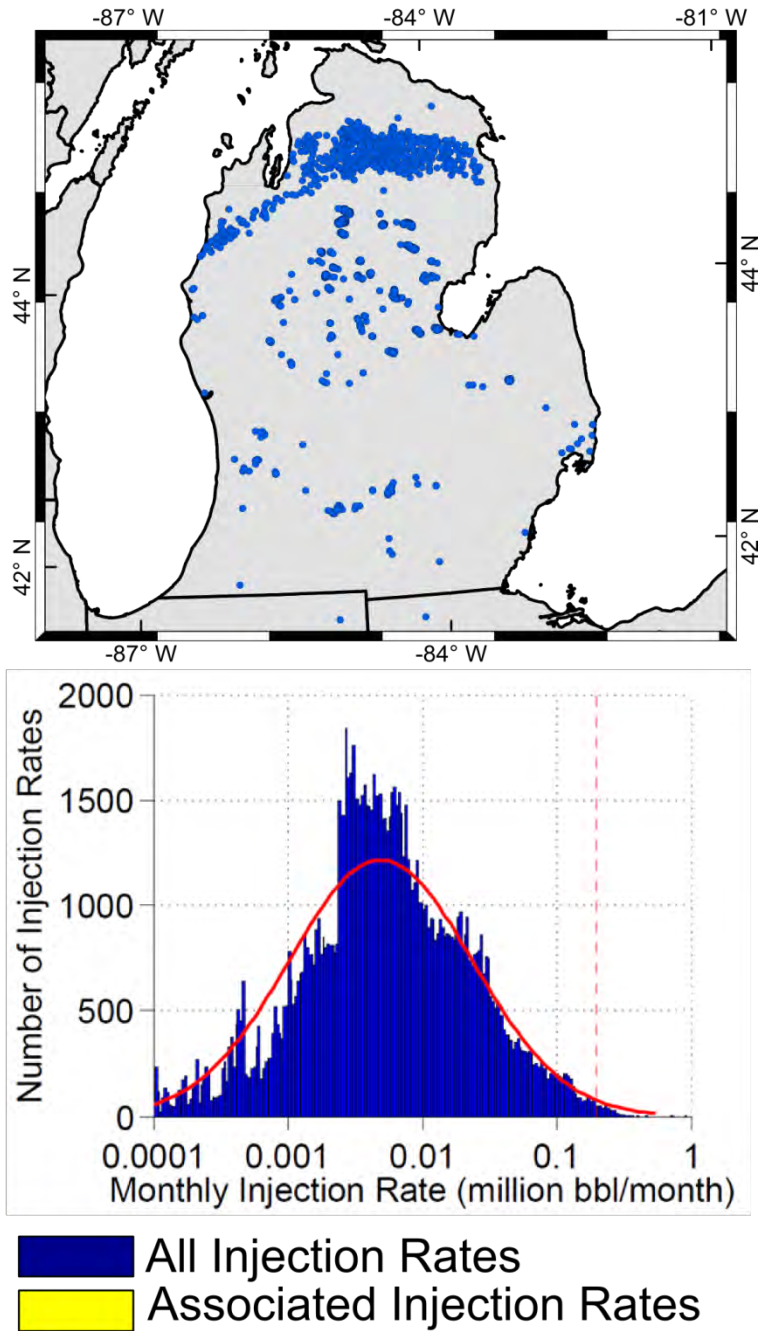


**Figure S18:** The spatial distribution of Class II injection wells in the Michigan Basin. There are no injection wells associated with seismicity in the entire Michigan Basin. The lower figure shows a histogram of injection rates for Class II wells in the Michigan Basin. The solid red line shows the Gaussian fit to the distribution and the dashed red line denotes the threshold of injection rates greater than 200,000 bbl/month. The mean injection rate of wells in Michigan is ~4,300 barrels/month, which is lower than that of other states with associated wells. However, more than 30 injection wells have maximum injection rates greater than 200,000 bbl/month.

**Table S1:** State-by-state list of injection well database sources and attributes.

State	Database Source Location	How were data acquired?	What data acquired?
Alabama	<a href="http://www.gsa.state.al.us/ogb/db_main.html">http://www.gsa.state.al.us/ogb/db_main.html</a>	Web Download Available	API, Well Type, Authorization Date, Latitude, Longitude, Well Status
Arkansas	<a href="http://www.aogc.state.ar.us/JDesignerPro/JDPArkansas/AR_Welcome.html">http://www.aogc.state.ar.us/JDesignerPro/JDPArkansas/AR_Welcome.html</a>	Web Download Available	API, Water Injection Permit, County Name, Well Name, Well Type, Latitude, Longitude, Depth To Be Drilled, DTD, Perforations Measured Depth, Well Status, Monthly Injection Volume, Monthly Injection Pressure
Colorado	<a href="http://cogcc.state.co.us/">http://cogcc.state.co.us/</a>	Web Download Available	API, Formation, Monthly Injection Volume, Monthly Injection Pressure, Well Status Date, Spud Date, Total Depth, Measured Depth, Perforations Top and Bottom, UTM Northing, UTM Easting, Latitude, Longitude
Florida	<a href="http://www.dep.state.fl.us/Water/mines/oil_gas/permit_data.htm">http://www.dep.state.fl.us/Water/mines/oil_gas/permit_data.htm</a>	Web Download Available	Permit Number, Well Type, Well Status, Completion Date, Plug Date, Total Depth, Latitude, Longitude
Illinois	<a href="http://maps.isgs.illinois.edu/iloil/">http://maps.isgs.illinois.edu/iloil/</a>	Manual web download using GIS server	API, Permit Number, Well Status, Latitude, Longitude, Injection Formation, Company Name, Elevation, Completion Date, Total Depth
Indiana	Closed Database	No online download available; state contact	Well Type, Completion Date, Max Pressure, Average Monthly Injection, Latitude, Longitude
Iowa	EPA has Primacy. Data not available on web.	No data could be acquired without FOIA. Only 7 Class II wells in all of Iowa.	None
Kansas	<a href="http://www.kgs.ku.edu/PRS/etroDB.html">http://www.kgs.ku.edu/PRS/etroDB.html</a>	Web Download Available	API, Kansas ID, Lease, Well, Field, Latitude, Longitude, Operator, Elevation, Depth, Permit Date, Spud Date, Completion Date, Plug Date, Well Type, Well Status
Kentucky	<a href="http://kgs.uky.edu/kgsweb/DataSearching/oilsearch.asp">http://kgs.uky.edu/kgsweb/DataSearching/oilsearch.asp</a>	Web Download Available	EPA_ID, Kentucky_ID, Company Name, Well Name, Well Class, Well Type, Well Status, Total Depth, Elevation, Injection Formation, Injection Top, Injection Bottom, Latitude, Longitude
Louisiana	<a href="http://sonris-www.dnr.state.la.us/gis/agsweb/IE/JSViewer/index.html?TemplateID=181">http://sonris-www.dnr.state.la.us/gis/agsweb/IE/JSViewer/index.html?TemplateID=181</a>	Manual web download using GIS server.	API, Well Serial, Well Name, Well Status, Well Description, Latitude, Longitude, Perforation Depths, Measured Depths

Michigan	<a href="http://www.michigan.gov/deq/0,4561,7-135-3311_4111_4231-214727--,00.html">http://www.michigan.gov/deq/0,4561,7-135-3311_4111_4231-214727--,00.html</a>	Web Download Available.	API, Well Name, Company Name, Permit Number, Well Type, Well Status, Latitude, Longitude, Monthly Injection Volume, Monthly Injection Pressure, Formation Tops.
Mississippi	<a href="http://gis.ogb.state.ms.us/M SOGBOOnline/">http://gis.ogb.state.ms.us/M SOGBOOnline/</a>	Web Download Available.	API, Well Type, Well Status, Well Name, Operator, Latitude, Longitude.
Missouri	<a href="http://www.dnr.mo.gov/geology/geosrv/ogc/index.html#permitted">http://www.dnr.mo.gov/geology/geosrv/ogc/index.html#permitted</a>	Web Download Available.	API, Well Type, Well Status, Company Name, Approval Date, Spud Date, Completion Date, Latitude, Longitude, Elevation, Total Depth, Perforation Depths, Formations.
Montana	<a href="http://boge.dnrc.mt.gov/WebApps/DataMiner/">http://boge.dnrc.mt.gov/WebApps/DataMiner/</a>	Web Download Available.	API, Company Name, Well Number, Well Status, Well Type, UIC Permit, Application Date, Effective Date, Max Pressure, Latitude, Longitude, Completion Date, Depth to be Drilled, Monthly Injection Volumes, Monthly Injection Pressure.
Nebraska	<a href="http://www.nogcc.ne.gov/NOGCCPublications.aspx">http://www.nogcc.ne.gov/NOGCCPublications.aspx</a>	Web Download Available.	API, County, Well Type, Well Status, Formation, Top Depth, Spud Date, Completion Date, Plug Date, Depth to be Drilled, Latitude, Longitude, Elevation
New Mexico	<a href="https://wwwapps.emnrd.state.nm.us/ocd/ocdpermitting/Data/Wells.aspx">https://wwwapps.emnrd.state.nm.us/ocd/ocdpermitting/Data/Wells.aspx</a>	Web Download Available.	API, Well Name, Well Number, Well Type, Well Status, Latitude, Longitude, Total Depth, Spud Date, Plug Date, Monthly Injection Volume, Monthly Injection Pressure
New York	<a href="http://www.dec.ny.gov/cfm/x/extapps/GasOil/search/wells/index.cfm">http://www.dec.ny.gov/cfm/x/extapps/GasOil/search/wells/index.cfm</a>	Web Download Available.	API, Formation Tops, Well Name, Well Type, Well Status, Status Date, Permit App Date, Permit Issue Date, Spud Date, Total Depth Date, Completion Date, Plug Date, Latitude, Longitude, True Vertical Depth, Measured Depth
North Dakota	<a href="https://www.dmr.nd.gov/oilgas/">https://www.dmr.nd.gov/oilgas/</a>	Web Download Available.	File Number, Well Name, Well Type, Well Status, Well Status Date, UIC Status, Date of First Injection, Last Report Date, Last PPSI, Last Monthly Injection, Cumulative Water Barrels, Max Allowed Pressure, Latitude, Longitude
Ohio	<a href="http://oilandgas.ohiodnr.gov/industry/underground-injection-control">http://oilandgas.ohiodnr.gov/industry/underground-injection-control</a>	State contact	API, Well Type, Latitude, Longitude, Deepest Formation, Total Depth, First Injection, Maximum Pressure, Permit Date, Conversion Date

Oklahoma	<a href="http://www.occpermit.com/WellBrowse/">http://www.occpermit.com/WellBrowse/</a> <a href="http://imaging.occeweb.com">http://imaging.occeweb.com</a>	Web Download Available.	API, Lease Name, Packer Depth, Latitude, Longitude, Monthly Injection Volume, Monthly Injection Pressure
Pennsylvania	Closed Database	Only SWD data available through EPA Contact	API, Facility ID, Facility Name, Injection Formation, Surface Injection Pressure Average, Average Monthly Injection Rate, Latitude, Longitude
South Dakota	<a href="http://www.sdgs.usd.edu/sd_oil/oilgas_databases.html">http://www.sdgs.usd.edu/sd_oil/oilgas_databases.html</a>	Web Download Available.	API, Facility ID, Well Name, Well Type, Well Status, Average Daily Injection rate, Injection Pressure Average, Injection Pressure Max, Latitude, Longitude, Permit Date, Completion Date, Plug Date
Tennessee	EPA Authority. Called but never received a response from district head.	FOIA Request Needed. Only 16 wells in entire state.	None
Texas	<a href="http://gis2.rrc.state.tx.us/public/startit.htm">http://gis2.rrc.state.tx.us/public/startit.htm</a>	Web Download Available.	API, Latitude, Longitude, Original Authority Date, Permit Cancel Date, Plug Date, Injection Type, Max Liquid Pressure, Max Liquid Volume, Top Injection Depth, Bottom Injection Depth
Virginia	Only about a dozen wells. All in western Virginia.	EPA contact	API, Facility ID, Facility Name, Injection Formation, Surface Injection Pressure Average, Average Monthly Injection Rate, Latitude, Longitude
West Virginia	<a href="https://apps.dep.wv.gov/oog/wellsearch_new.cfm">https://apps.dep.wv.gov/oog/wellsearch_new.cfm</a>	Web Download Available.	API, Permit Type, Permit Issue Date, Operator, Formation, Well Status, Well Type, Latitude, Longitude
Wyoming	<a href="http://wogcc.state.wy.us/">http://wogcc.state.wy.us/</a>	State contact	API, Latitude, Longitude, First Injection Date, Monthly Injection Volumes, Monthly Injection Rate, Total Depth



**Table S2:** Cases of documented and suspected induced seismicity from EPA Class II wells used to test the spatiotemporal filter.

Site	Date	Maximum Earthquake Magnitude	Reference Number	Spatiotemporal Filter
Painesville, OH	1/31/1986	5	15	Yes
Youngstown, OH	12/31/2011	4	18	Yes
Raton Basin, CO	9/5/2001	4.5	40	Yes
Raton Basin, CO	8/23/2011	5.3	10	Yes
Jones, OK	4/16/2013	4.4	24	Yes
Prague, OK	11/6/2011	5.6	8	Yes
Cogdell, TX	6/16/1978	4.4	41	Yes
Cogdell, TX	9/11/2011	4.3	42	Yes
Dagger Draw, NM	12/19/2005	4.1	43	Yes
Timpson, TX	5/17/2012	4.8	11	Yes
El Dorado, AR	12/9/1983	3	44	Yes
Guy, AR	2/28/2011	4.7	12	Yes
Southern Alabama	10/24/1997	4.9	45	Yes
Kermit Field, TX	1/19/1976	3.5	41	Yes
Hunt Field, MS	5/4/1977	3.6	41	Yes
Rangely, CO	3/19/1979	3.3	41	Yes
Sleepy Hollow Field, NE	7/16/1979	3.2	41	Yes

**Table S3:** Test of Mooney and Kaban (2010) sediment thickness depths against known reference depths in several regions across the CEUS where the proximity to basement calculation is made.

<b>Test Site</b>	<b>Latitude</b>	<b>Longitude</b>	<b>Reference Depth (km)</b>	<b>Mooney-Kaban Depth (km)</b>	<b>Residual (km)</b>	<b>Percent Error</b>	<b>Reference Number</b>
<b>Youngstown, OH</b>	41.12	-80.68	2.74	3.15	0.41	14.96	18
<b>Denver, CO</b>	39.85	-104.86	3.64	3.56	-0.08	-2.20	1
<b>Jones, OK</b>	35.40	-97.44	3.51	3.08	-0.43	-12.13	24
<b>Paradox Valley</b>	38.21	-108.88	4.71	5.16	0.45	9.62	38
<b>Williston Basin West</b>	48.00	-104.00	4.58	4.76	0.18	3.93	39
<b>Williston Basin East</b>	48.00	-99.00	1.15	1.10	-0.05	-4.35	39
<b>Timpson, TX</b>	31.87	-94.45	5.00	5.41	0.41	8.20	11
<b>Michigan Basin</b>	43.45	84.38	4.97	4.93	-0.04	-0.80	46

**Table S4:** Suspected mining blasts removed from the ANSS catalog prior to the earthquake-injection well spatiotemporal filter. Data provided by Susan Hoover, U.S. Geological Survey, Golden, CO.

Date	Latitude	Longitude	Depth (km)	Magnitude	ANSS Catalog Type
<b>Decker Coal Mine, MT</b>					
2/13/2013	45.0729	-106.7529	0	3	earthquake
<b>Rock Springs, WY</b>					
2/13/2013	41.7862	-108.6866	0	3.3	earthquake
8/14/2013	41.7322	-108.763	-2.7	2.7	earthquake
7/19/2013	41.2462	-108.7898	-3.1	2.9	earthquake
<b>Kemmerer, WY</b>					
1/2/2013	41.71	-110.69	0	2.7	earthquake
2/27/2013	41.735	-110.6465	0	2.6	earthquake
<b>Located AT Powder River Basin, WY</b>					
5/10/2013	43.785	-105.452	5	2.5	earthquake
1/24/2013	43.809	-105.199	0	3.4	earthquake
5/11/2013	43.7425	-105.2197	0	3.4	earthquake
1/17/2013	43.6205	-105.2341	0	3.2	earthquake
1/2/2013	43.829	-105.254	0	2.8	earthquake
<b>Located near Powder River Basin, WY</b>					
3/18/2013	43.4994	-106.0245	0	3.1	earthquake
<b>Located near Powder River Basin, WY</b>					
1/3/2013	43.986	-105.086	0	3.1	earthquake
<b>Located close to coal mines in Alabama</b>					
6/22/2013	33.621	-87.178	0	2.6	earthquake
<b>Felt event near Grants, NM</b>					
6/14/2013	35.136	-107.736	0	3.4	earthquake